2007

Influence of tumor necrosis factor-alpha and minocycline on microglia and macrophage activation during polytropic retrovirus infection

Meryll E. Corbin
Louisiana State University and Agricultural and Mechanical College

INFLUENCE OF TUMOR NECROSIS FACTOR-ALPHA AND MINOCYCLINE ON MICROGLIA AND MACROPHAGE ACTIVATION DURING POLYTROPIC RETROVIRUS INFECTION

A Thesis

Submitted to the Graduate Faculty of the
Louisiana State University and
Agricultural and Mechanical College
in partial fulfillment of the
requirements for the degree of
Master of Science

in

The Interdepartmental Program in Veterinary Medical Sciences
through the
Department of Pathobiological Science

by
Meryll E. Corbin
B.S., Animal Science, 2004
May 2007

Acknowledgements

I would like to take this opportunity to sincerely thank my Master's Thesis committee, Drs. Stephania Cormier, K. Gus Kousoulas, and Karin Peterson, for going above and beyond their requirements as committee members and asking only that I perform to the best of my ability in return. At this time, I really must give a lot more credit to Dr. Karin Peterson. She gave me an excellent opportunity to not only learn and grow as a budding scientist, but also to contribute to the greater good of research. And for this, I will always be grateful.

I would next like to acknowledge the members of the Peterson Laboratory, past and present, who have had to deal, and perhaps not so willingly, with my eclectic taste in music and my tendency to burst into song, particularly: Susan Pourciau, Stephanie Lewis, Lauren Duhon, Min Du, Mohammed Khaleduzzaman, Niranjan Butchi, and Trey Brown. I cannot forget to mention the Vixens of the Vet School: Katie Reif, Erica D'Spain, and Trisha Olivier. These fine ladies have just been wonderful listeners and friends in all things science and shoes. I also have to thank both Tom and Theresa Olivier for being my surrogate parents during my first year here. They and their extended family welcomed me with open arms and a full plate when I was oh so very far away from home.

My friends away from home have been such a stabilizing factor during my time here: Jenn McRobbie, Kate Nestor, and Mary Cloutier. To my family, Mom, Dad, Beebz, and Sissy: you may not understand what I do or why I do it but you have questioned neither my commitment nor my decisions. Besides, getting treated like a hero because I only got home twice a year never got old. To poochy: without you, I probably would never have finished as an animal science major, never interned, and never decided to go to graduate school. So wherever you are, may you always have a cat to chase and a warm fireplace to sleep beside.

The entire Pray family has just been so wonderful and accepting of this crazy Northerner. I have learned so much about Louisiana history and Southern culture just from asking questions that y'all were always willing to answer. And that brings me to the final person that I need to acknowledge. Oh, Derek. Our chance meeting has turned my life completely inside-out, but in a good way. You have always eaten whatever I have cooked and said it was great, indulged some of more ridiculous fancies (like going to three different stores just to find Cape Cod potato chips), and said that you liked to see me smile. Well, I am certainly smiling now and whatever challenges may come our way I will continue to smile as long as I have you by my side to continue to keep me humble and love me like no one else has.

Table of Contents

Abstract

Microglia/macrophage activation has been associated with the pathogenesis of various neurological diseases including human immunodeficiency virus encephalitis, transmissible spongiform encephalitis, and Alzheimer's disease (AD). *In vitro* studies have indicated a role for TNFα in activating these cells which leads to their migration, proliferation, and secretion of proinflammatory cytokines and chemokines that may potentially damage brain tissue. In the current study, we analyzed the phenotype of microglia and macrophages enriched from wild type and TNFα deficient mice infected with a neurovirulent murine retrovirus. Although TNF receptors CD120a and CD120b were expressed on both microglia and macrophage population, unaltered by either retrovirus infection or TNFα deficiency. To determine if hindering microglia/macrophage activation and TNFα expression during an established viral infection would impede the development of neurological disease, we treated mice with minocycline which has been reported to inhibit both microglia activation and TNFα production. Despite the decreased expression of certain genes involved in TNF signaling and microglia/macrophage activation, there was no delay in onset of neurological disease between PBS and minocycline treated EC infected mice. mRNA expression for accessory molecules involved in the TNF Superfamily signaling was significantly reduced with minocycline treatment. Understanding how to better manipulate these pathways could lead to ways to decrease the severity of neurological disease in not solely this model but others in which they has been directly linked to pathogenesis.

Chapter 1: Introduction

HIV infection of the central nervous system is observed in 80% of those infected with HIV, spreading presumably by infected monocytes, macrophages or T cells. However, only 20% of HIV infected individuals develop neurological disease[1]. The cytokine tumor necrosis factor-alpha (TNFα) has been implicated in disease progression in patients suffering from HIV-associated dementia[2], based on studies involving gene expression of patients with and without dementia[3,4]. However, the mechanism by which TNFα is acting in pathogenesis has yet to be elucidated. In a study involving a neurovirulent retrovirus, animals deficient in TNFα had either delayed disease or no symptom presentation when infected[5], indicating a role for TNFα in pathogenesis. In the same study, decreased expression of the microglia/macrophage activation marker F4/80 was also observed in infected TNFα deficient animals when compared to infected wild type animals, indicating the lack of TNF may be having an effect on microglia/macrophage activation[5].

Microglia can be activated by direct interaction with viruses, bacteria, or cytokines[2,6,7]. Activation of these cells leads to their migration, proliferation, and secretion of TNFα and IL-1β and other proinflammatory cytokines and chemokines which may potentially damage brain tissue[8]. Therefore, we hypothesize that TNFα may be important for the activation of microglia/macrophages during retroviral pathogenesis in the brain. In the present study, we analyzed the effect of TNFα on the microglia and macrophage response to retrovirus infection in the brain using a mouse model of polytropic retrovirus infection. We enriched microglia and macrophages from retrovirus infected wild type (WT) and TNF-/- mice to analyze the activation state of these cells during infection. In addition, we treated EC infected mice with the microglia activation inhibitor minocycline to determine if administration after the establishment of a

productive viral infection influenced the onset of neurological disease that may be attributed to microglia activation and TNFα secretion.

Chapter 2: Review of Literature

2.1: Tumor Necrosis Factor-Alpha (TNFα)

First observed in the mid 1800s, TNFα has long been associated with immunological function and more recently pathogenesis. TNFα belongs to a family of structurally related molecules that are involved in cell signaling and immune responses. TNFα is produced by numerous cell types including natural killer cells, monocytes/ macrophages, and lymphocytes. TNFα is initially synthesized and expressed as a transmembrane molecule, the extracellular portion of which is subsequently cleaved by TNFα converting enzyme (TACE) to release the soluble 17 kDa molecule[9]. Originally, it was believed that TNFα was more potent in its soluble form, but current studies indicate that the membrane bound form has a crucial role in cell to cell signaling whereas the soluble form of the cytokine may be more involved in apoptosis[10].

2.2: TNFα and Neurological Disease

TNFα upregulation has been associated with the pathology of many neurological diseases including multiple sclerosis (MS)[11], Alzheimer's disease (AD)[12], transmissible spongiform encephalopathy [13-15] and HIV associated dementia [2,16-18], but the exact mode in which TNFα contributes to disease *in vivo* has yet to be established. TNFα and TNF- receptor (TNFR) neutralization studies have met with mixed success[11]. In a study involving a TNFR1 blocking agent to treat the symptoms of MS, most patients reported reduced symptoms, but some experienced exacerbations during the trial[11,19]. In an extreme case, the systemic anti TNFα treatment induced symptoms similar to lupus in trial participants[20].

2.3: TNFα and Human Immunodeficiency Virus associated Dementia

TNFα involvement may contribute to the pathogenesis of HIV in the brain. For example, the TNFα 308 allele had a much greater occurrence in those suffering with HAD, suggesting the

potential for a genetic predisposition to developing the disease[21]. The distribution of apoptotic neurons in HIV patients was closely associated with the presence of activated microglia[16]. Reports of elevated levels of TNFα and TNFR expression in microglia/macrophage isolated from individuals suffering from HAD[3] suggest that soluble factors released by these activated cells may be important in mediating neurotoxicity. The finding that neurons have the pro-apoptotic TNFR1 on their cell surface supports the hypothesis that TNFα secreted by activated microglia or macrophages may induce neuronal apoptosis[3]. Immunohistochemical analysis of brain tissue from patients with HAD displayed a correlation between severity of disease and TNFα and NFκB expression[16]. TNFα also serves to stimulate the release of excitatory amino acids (EAAs), most notably L- cysteine, which may act to stimulate neuronal apoptosis via N-methyl-D-aspartate receptors (NMDARs)[22].

2.4: TNF Superfamily Receptors and Signaling

TNFα binds to two receptors: CD120a (p55-R, TNF-R-I p55, TNF-R, TNFR1, TNFAR, TNF-R55, p55TNFR, TNFR60, *Tnfsfr1a*) and CD120b (p75, TNF-R, TNF-R-II, TNFR80, TNFR2, TNF-R75, TNFBR, p75TNFR). The receptors are single transmembrane glycoproteins with 28% homology mainly residing in their extracellular domain consisting of four tandemly repeated cysteine-rich motifs[10]. They are coexpressed on the surface of most cell types, with the smaller CD120a associated with the traditional TNFα associated inflammatory responses and apoptosis whereas the CD120b receptor has been implicated in T cell apoptosis, TNFα induced skin necrosis, and thymocyte proliferation[23]. The CD120a:CD120b expression ratio of a certain cell may predetermine the response of the cell to TNFα.

CD120a serves to recruit TNFR1 associated death domain protein (TRADD) which can in turn recruit receptor interacting protein-1 (RIP1) or Fas-associated death domain protein

(FADD) (fig. 1) (rev in [17]). RIP1 interacts with antiapoptotic proteins which serve to activate the MAP kinase pathways ultimately leading to the activation of the transcription factor NFκB. Thus activated, NFκB aids in promoting cell survival. Conversely, the interaction of FADD with TRADD recruits pro-caspase 8, thus forming the death- inducing signaling complex (DISC). This cleaves the caspase, thereby forming its active form which triggers the downstream activation of effector caspases [24] which will subsequently lead to cell death.

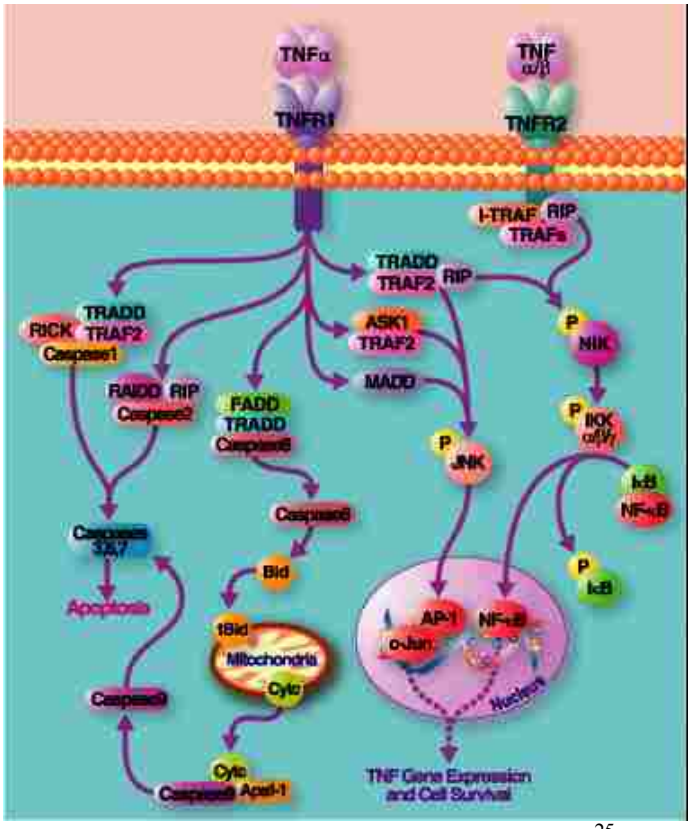

Figure 1: Signaling pathways of CD120a (TNFR1) and CD120b [25]. Taken from http://www.biotechjournal.com/Journal/jan %202002/jan Article 6text.htm

Activation of the other TNFα receptor CD120b initially leads to the recruitment of TRAF2 (fig. 1) (rev. in [17]). Ultimately, the downstream action of this is to activate NFκB and promote cell survival. Certain limitations exist when studying signal transduction via CD120b. Upon activation the receptor is readily autolytically cleaved from the cell surface. Possibly, the cleaved form may serve a decoy function[26]. In this soluble form, CD120b retains the ability to

bind cytokine. The membrane form of TNFα has a much higher affinity for CD120b, indicating that this receptor may play an important role in cell to cell communication rather than apoptosis.

Although TNF does not signal through CD95, TNFR1 and CD95 share a similar signal transduction pathway that can interact with each other. CD95 (FAS, APO-1, APT1, *Tnfsfr6*) is synthesized as a transmembrane protein that forms a trimeric complex to induce signaling (rev. in [26]). CD95 is expressed on a variety of cell types while CD95L expression is restricted to immune cells including NK cells and activated T cells. Similar to TNFR1, CD95 contains a death domain (DD) which allows adaptor proteins to dock and initiate signaling. One such protein is CD95-associated protein with DD (FADD), which interacts with Daxx to initiate apoptotic signals by activating caspase cascades or other pathways. In addition, alternative splicing of the CD95 mRNA will produce decoy receptors that lack the DD and thereby inhibit CD95 mediated signaling. CD95 and CD95L have been reported to be elevated in several neurological conditions including retrovirus neurodegeneration, Alzheimer's, Huntington's, and Parkinson's disease[27-30].

2.5: Microglia/Macrophages and TNFα

One of the ways in which TNFα may be involved in neurological disease is through its ability to activate mircoglia[31]. The presence of TNFα correlates with microglia/macrophage activation or recruitment[31]. The secretion of TNFα early in spinal cord injury may be involved in autoactivating microglia/macrophages[32]. Studies indicate a role for TNFα in accentuating monocyte/ macrophage recruitment to sites of viral infection[33], potentially spreading the virus within the brain if the cells are actively infected. A study involving TNFα knockout mice reported decreased mRNA expression of the microglia/macrophage activation marker *F4/80* during neurovirulent retroviral infection as compared to wild type controls[5]. This lack of

activation may have slowed or completely halted disease progression in these animals, for only 15% of animals infected developed neurological symptoms[5]. Therefore, elucidating this detailed activation process may give researchers more insight into how to halt or delay this process and potentially hinder activated microglia/macrophage induced neurological disease.

2.6: Microglia

Microglia cells support and protect neurons and serve to facilitate the innate immune response within the CNS. In the brain, there are two distinct types of cells hailing from the hemopoietic lineage: parenchymal microglia, perivascular or meningeal macrophages. Microglia perform tasks including maintenance of homeostasis, production of nerve growth factors and neurotrophins thus aiding in the removal of dead cells and the regeneration of damaged neurons[18]. Under normal conditions, parenchymal microglia are present in a ramified or highly processed form where they have low phagocytic and endocytic activity. When resting, they interact with astrocytes and neurons in signaling and support. Activation causes them to retract their processes and shift into a more amoeboid or macrophage-like morphology[34,35]. In addition to morphology modifications, gene expression profiles of activated microglia also change[8,36-38] with recent evidence suggesting that these alterations are stimulus specific[38]. Acquired functions of activated microglia include increased expression of innate immune cell surface receptors including Fc receptors and pattern recognition, proliferation, migration, and increased secretion of proinflammatory mediators including TNFα and IL-1β, as well as generation of reactive oxygen intermediates and nitrogen intermediates[39]. This microglia/macrophage activation may potentially precede neuronal death, which was demonstrated in experiments showing that apoptosis in neurons was found following the activation of microglia during prion disease[40].

Cell surface markers have proven useful in differentiating activated from resting microglia[5]. Microglia have been molecularly phenotyped using cell surface markers. For example, F4/80, CD11b/c and CD45 are commonly used to identify and describe microglia[5,41-43]. F4/80 can be used to determine the degree of microglia activation for it is upregulated upon activation[44]. Additionally, ionized binding calcium adapter molecule (Iba1) has been used as a general marker for immunohistichemical identification of microglia[45,46]. The expression level of CD11b (Mac-1) and CD45 differ based upon the state of activation. CD45 is also used to identify macrophages, but the expression of this marker by microglia is approximately one half that of tissue macrophages[47] allowing this marker to be used to differentiate between $CD45^{hi}$ CD11b+ macrophages and $CD45^{lo}$ CD11b+ microglia[43].

2.7: Microglia/Macrophages and Retrovirus Infection

The principal pathogenesis of HAD appears to involve the response of microglia and infiltrating macrophages. Early in disease, few microglia are productively infected with HIV whereas later in disease the majority of infected cells tend to be parenchymal microglia[48]. In HAD patients, microglia are proposed to serve both a neuroprotective and potentially neurodegenerative role. When retrovirus replication occurs in the brain, it can activate macrophages and microglia leading to the upregulation of adhesion molecules and chemokines in the microvascular endothelial cells thereby further breaking down the blood brain barrier and allowing for increased cellular traffic into the brain[49]. Microglia can be activated by the virus itself, by indirect immune stimulation, or by interacting with secreted viral proteins[50]. Microglia activation leads to an upregulation of their effector molecule production many of which may potentially harm the brain. Proinflammatory cytokines, proteases, excitatory amino acids and oxide radicals released by microglia may serve to damage CNS tissue[51]. Therefore,

understanding the signaling involved in microglial activation is crucial for the development of therapeutics for the treatment and prevention of HAD.

2.8: Microglia and Other Neurological Diseases

In addition to HAD, microglial involvement or activation has been associated with the pathology of many neurological diseases including AD, MS, and TSE. Microglia cultured from patients suffering from AD show increased chemotaxis towards beta- amyloid protein plaques, and increases in both activation and phagocytic activity[52]. During the early stages of MS, microglia display increased proliferative and lysosymal activity[53]. During TSE infection, infected microglia display phenotypic changes and distinct pattern of inflammatory molecular changes[38].

2.9: Inhibition of Microglia/macrophage Activation

Minocycline (7-Dimethylamino-6-demethyl-6-deoxytetracycline) is part of the tetracycline family of antibiotics, sharing broad spectrum antibiotic capabilities[54]. Tetracyclines act upon bacteria by inhibiting protein synthesis (for a rev., see Ref. 55). Minocycline is structurally different from the basic tetracycline in the location of a single amino group (Fig. 2). In humans, the drug is either administered orally or intravenously with dosage recommendations the same for either route whereas researchers in animal studies usually inject it intraperitoneally for *in vivo* testing[54,56]. The drug is rapidly and readily absorbed leading to less disruption of the natural gastrointestinal flora[54]. A distinct advantage of minocycline is its lipophilic nature, thereby enhancing diffusion into the tissue, including the brain[57]. Minocycline has been shown to interfere with inflammatory responses due to its role in hindering microglia activation.

Recently, minocycline has been reported to interfere with inflammation in Alzheimer's Disease[58], global and focal ischema[58,59] certain models of Huntington's disease[60-62], and

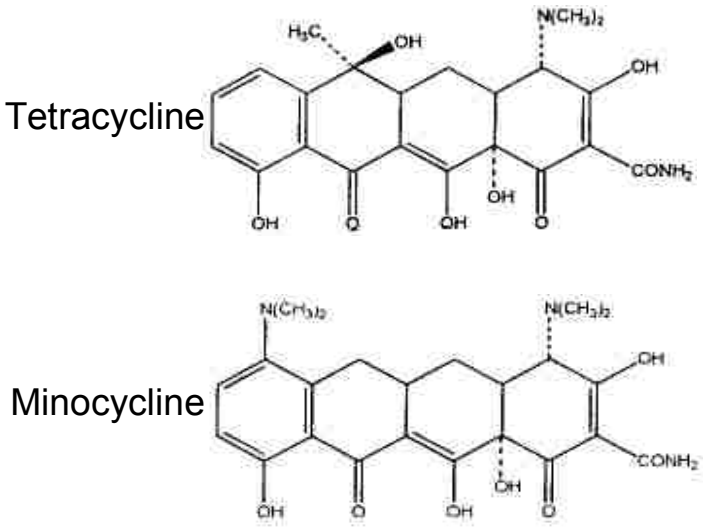

Figure 2: The structure of minocycline differs from that of a basic tetracycline in a single amino group[55].

simian immunodeficiency virus[63]. In most of these cases, activation of microglia was also severely inhibited[57-59,63-66], thereby reducing the release of iNOS, NADPH oxidase, and inflammatory mediators including cytokines and chemokines, including TNFα[2]. In certain animal models of Huntington's disease, release of caspases-1 and -3 was reduced potentially interfering with apoptosis. In addition, cytochrome *c* release from mitochondria was also decreased when animals were treated with the drug[56]. A recent report illustrates minocycline's ability to inhibit TNFα expression in mixed glia cultures and promote neuronal survival[64]. Researchers have recently reported that minocycline proved useful in attenuating or potentially inhibiting encephalitis in a macaque model of SIV[63]. The same study also revealed a significant decrease in levels of monocyte chemoattractant protein-1 [67] as measured by enzyme-linked immunosorbent assay in animals treated with minocycline[63].

2.10: Murine Model

Certain fields of science have grown tremendously through the use of an animal model to study biological effects. Cell culture models may mimic the activity of a certain cell type, but

they cannot truly match the response achieved in the dynamic environment of living tissue. The murine model allows for the manipulation of the host genetics in order to determine the role of specific gene products in disease progression.

Murine leukemia viruses [27] are a group or retroviruses that induce a number of diseases. Polytropic retroviruses induce a neurological disease consisting of tremors of the hind limbs, ataxia, and seizures[5,68]. Polytropic retroviruses differ from the more commonly studied ecotropic retroviruses in that their envelope protein binds to xenotropic polytropic receptor- 1 (XPR1) as a cellular receptor rather than cationic amino acid transporter-1 (CAT-1) used by ecotropic viruses[69]. The envelope protein has been shown be a factor in mediating neurological disease. For example, the Fr98 virus was initially constructed by inserting a portion of the polymerase and the entire envelope gene of a neurovirulent virus [70] into the non-neurovirulent FB29 virion[71]. Fr98's envelope gene contains two separtate neurovirulent determinants: between the EcoRI to ClaI (EC)and the BbsI to EcoRI (BE) restriction enzyme digestion sites[70] (Table 1). All viruses infect the same cell types including microglia and endothelia and are present in similar regions of the brain[70,71].

The EC region of the Fr98 envelope gene is known to induce the same neurological symptoms as Fr98, but with slower progression and decreased incidence[5]. Increased expression of proinflammatory cytokines and chemokines are associated with this model of neurological disease[72]. The lack if lymphocyte infiltration seen in this model suggests that the innate immune system is responsible for the chemokine/ cytokine changes. The characteristic pathology associated with this disease is activation of astrocytes and the activation or recruitment of macrophages/ microglia[72]. EC infection leads to an upregulation of TNFα in infected wild type

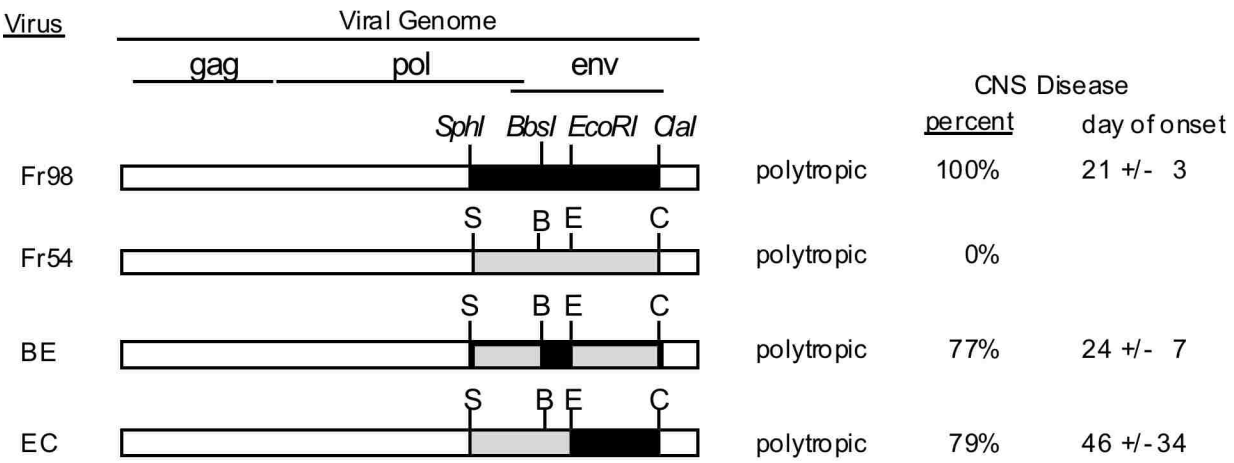

Figure 3: A depiction of the virus genomes for the parent and chimeric strains with corresponding incidence of neurological disease in 129SvEv mice[72].

animals, indicating a role for the presence of TNFα in EC induced pathogenesis. In 129SvEv mice, disease presented as early as day 20 with 50% clinical by day 25 post infection and with 79% of animals becoming clinical by the termination of the study[5]. EC virus infection in TNF-/- animals induced disease in 15% of animals by the termination of the study.

Microglia/macrophage activation, as measured by *F4/80* mRNA expression, was dramatically decreased in EC infected TNF-/- animals[5] indicating that the presence of TNFα may be necessary for microglia/macrophage activation during EC infection. In the current study, we analyzed how decreased or an absence of TNFα influences microglia/macrophage activation and TNFα signaling.

Chapter 3: Materials and Methods

3.1 Solutions

10x Phosphate buffered saline (PBS)

26.8 g Sodium phosphate, dibasic

13.8 g Sodium phosphate, monobasic

75.6 g Sodium chloride

Dissolve in 800 ml ddH_2O

Adjusted pH to 7.0.

Brought to 1L with ddH_2O.

Stored at room temperature (RT).

1x PBS

100 ml 10x PBS

900 ml ddH_2O

Mixed completely and stored at RT.

10x Tris buffered saline (TBS)

24.2 g Tris base

87.7 g Sodium chloride (NaCl)

Dissolve in 800 ml ddH_2O

Adjusted pH to 7.5.

Brought to 1 L with ddH_2O.

Stored at RT.

1x TBS

100 ml 10x PBS

900 ml ddH_2O

Mixed completely and stored at RT.

0.1 M Citric Acid

1.92 g Citric acid, anhydrous

100 ml ddH_2O

Mixed completely and stored at RT.

0.1 M Sodium citrate, dihydrate

14.7 g Sodium citrate

500 ml ddH_2O

Mixed completely and stored at RT.

Citrate Buffer Antigen Retrieval Working Solution

9 ml of 0.1 M Citric acid

41 ml of 0.1 M Sodium citrate, dehydrate

Bring to 500 ml with ddH_2O.

Bring pH to 6.0.

Mixed completely and stored at RT.

Normal Donkey Serum Blocking Solution

2 ml donkey serum (Sigma)

1ml BSA (Sigma)

0.1 ml cold fish skin gelatin (Sigma)

0.1 ml Triton X-100 (Sigma)

0.05 ml Tween 20 (Bio-Rad)

98 ml 1x PBS

Mixed well and stored at 4°C.

DAPI Concentrated Stock Solution (5mg/ml or 14.3 mM)

10 mg 4',6-Diamidino-2-phenylindole (DAPI) (Invitrogen)

2 ml Dimethylformamide (DMF) (Fisher)

Vortexed to mix.

Aliquotted and stored at -20°C.

DAPI Working Solution (100ng/ml or 300nM in PBS):

2 µl DAPI Stock Solution

100 ml PBS

Wrapped bottle in foil to prevent light penetration. Stored at 4°C.

70% Percoll

70 ml Percoll (Sigma)

10 ml 10x PBS

20 ml ddH_2O

Mixed well and stored at 4°C.

37% Percoll

37 ml Percoll

10 ml 10x PBS

53 ml ddH_2O

Mixed well and stored at 4°C.

30% Percoll

30 ml Percoll

10 ml 10x PBS

60 ddH_2O

Mixed well and stored at 4^{o}C.

2% BSA/PBS

2 g bovine serum albumin (Sigma)

100 ml 1x PBS

Let the BSA sit on top of the PBS to dissolve. Mixed well and stored at 4^{o}C.

2% BGS/PBS

2 ml Bovine growth serum (BGS) (Biomeda)

98 ml 1x PBS

Mixed well and stored at 4^{o}C. Discard when solution appears cloudy.

0.5% FSG/TBS

5 ml cold fish skin gelatin (Sigma)

1 L 1 x TBS

Mixed well and stored at 4^{o}C. Discard when solution appears cloudy.

1% saponin/10xPBS

0.5 g saponin (Sigma)

50 ml ddH_2O

Let the saponin sit on top of the PBS to dissolve. Mixed well and stored at 4^{o}C.

0.1% saponin/PBS

5 ml 1% saponin/10xPBS

45 ml ddH_2O

Mixed well and stored at 4^{o}C.

2% Paraformaldehyde/PBS

2 g paraformaldehyde (Sigma)

100 ml 1x PBS

Dissolve at 56^{o}C while shaking.

Will take some time to dissolve. Mixed well and stored at 4^{o}C.

3.2: Antibody Information

Table 1: Information detailing primary antibody antigens, isotypes, source and concentration used in this study.

Antigen	Clone	Isotype	Vendor	Conjugation	Concentration	Working Dilution
CD11b	M1/70	Rat IgG2b, κ	BD Pharmingen	PE	0.2 μg/ml	1:1000
CD11c	HL3	Armenian Hamster IgG1, λ2	BD Pharmingen	FITC	5 μg/ml	1:200
CD14	mC5-3	Rat (LOU) IgG1, κ	BD Pharmingen	FITC	5 μg/ml	1:200
CD16/CD32	2.4G2	Rat (Sprague-Dawley) IgG2b, κ	BD Pharmingen	n/a	0.5 μg/ sample	1:200
CD45	30-F11	Rat (LOU/Ws1/M) IgG2b, κ	BD Pharmingen	FITC	5 μg/ml	1:200
CD45	30-F11	Rat (LOU/Ws1/M) IgG2b, κ	BD Pharmingen	PerCP	5 μg/ml	1:200
CD80	16-10A1	Armenian Hamster IgG2, κ	BD Pharmingen	PE	5 μg/ml	1:200
CD86	GL1	Rat (Louvain), IgG2b, κ	BD Pharmingen	PE	5 μg/ml	1:200
CD120a	HM104	Rat IgG2a	Serotec	R-PE	10 μl/sample	1:10
CD120b	HM102	Rat IgG2a	Serotec	R-PE	10 μl/sample	1:10
F4/80	BM8	Rat IgG2a, κ	eBioscience	FITC	2.5 μg/ml	1:200
F4/80	BM8	Rat IgG2a, κ	eBioscience	APC	2.5 μg/ml	1:200
CD68	FA-11	Rat IgG2a	Serotec	n/a	10 μg/ml	1:100
CD4	RM4-5	Rat (DA) IgG2b, k	BD Pharmingen	R-PE	5 μg/ml	1:200
CD8	53-6.7	Rat (LOU/Ws1/M) IgG2b, κ	BD Pharmingen	R-PE	5 μg/ml	1:200
gp70	n/a	Goat polyclonal	Rocky Mountain Labs	n/a	n/a	1:500
Iba-1	n/a	Rabbit polyclonal	Wako Scientific	n/a	2.5 μg/ml	1:200

3.3: Mouse Strains

129S6, (129SvEv), mice were purchased from Taconic (Hudson, NY). TNF-/- and wild-type controls (129S6) were kindly provided by Francis Balkwill and have been previously

described [73]. Animals were bred and maintained at the Louisiana State University School of Veterinary Medicine vivarium. All animal experiments were carried out under the guidance of Louisiana State University's Animal Care and Use Committee and the guidelines set forth by the National Institutes of Health.

3.4: Virus Infection

The construction of virus clone EC has been described previously [70]. Virus stocks were obtained from cell culture supernatants of cultured EC infected *Mus dunni* cells. Viral titers were determined by focus forming assays using the monoclonal antibody 720 which recognizes the viral envelope protein[70,74]. Neonates were inoculated within 24 hours of birth with 10^4 focus forming units (FFU) of EC in 100 µl of cell culture medium by intraperitoneal injection using a 27 ½ gauge needle and 1 ml syringe (Becton Dickinson, Franklin Lakes, NJ). Animals were observed daily for overt signs of clinical disease which was characterized by tremors of the hind limbs, ataxia and seizures. At the onset of neurological disease or at the appropriate time point, animals were euthanized under deep Isofluorane anesthesia followed by exsanguination with an axillary incision. Brains and spleens were removed and divided in half sagittally with half immersion fixed in 3.7% neutral buffered formalin (NBF) for 48 hours and kept in 70% ethanol until histological processing and the other half flash frozen in liquid nitrogen and stored at -80^{o}C for RNA isolation. For microglia enrichment, brains were removed and placed in ice cold 2% bovine growth serum (BGS)/ 1xPBS (2%BGS/PBS) in one well of a six well plate and kept on ice.

3.5: Minocycline Treatments

Litters of 129S6 were randomly assigned to one of four groups and inoculated as mentioned above. The four groups were as follows: mock infection and phosphate buffered

saline (PBS) treatment, mock infection and minocycline treatment, EC infection and PBS treatment, and EC infection and minocycline treatment. Starting on day 14 post infection and continuing every other day until the termination of the study, litters were weighed on a digital scale (Ohaus, Pine Brook, NJ) and injected with 35 mg of minocycline per kg of body weight in PBS for a total volume of 20 µl per animal. Animals were weighed at each injection until they reached a constant weight at which point they were weighed weekly. Minocycline was administered with a single intraperitoneal injection using a 29 gauge insulin syringe (BD). Animals were monitored daily for signs of neurological disease and euthanized as described above.

3.6: Enrichment of Microglia

Prior to each experiment, Percoll step gradients were generated to contain 2.5 ml 30% and 2.5 ml 37% layers in 15 ml tubes. In some experiments, trypan blue (0.04% trypan/37% Percoll) and/or phenol red (0.4% Phenol red/70% Percoll) (Sigma, St. Louis, MO) were added to more readily define the layers. At the appropriate time post infection, brains were removed and kept on ice until processing. Tissues were disrupted in a sterile glass dounce homogenizer using 7-9 strokes. The homogenate was removed with a sterile transfer pipette and placed in a sterile 15 ml tube (Biologix), the homogenizer washed with approximately 6 ml of ice cold PBS and added to the original homogenate. Samples were centrifuged at 1500 rpm for 10 minutes at 4^{o}C, supernatants were poured off, and the pellet was resuspended in 5 ml 70% Percoll/ 1xPBS. The homogenate was pipetted under two pre-made 30%/ 37% Percoll gradient and centrifuged at 500 x g for 20 minutes at room temperature with no brake. Lesser dense brain tissue migrated to the upper levels of the gradient and was discarded. The cells between the 37%/ 70% layer were collected and pelleted at 1500 rpm for 10 minutes at room temperature. Any remaining

erythrocytes were lysed with red blood cell lysis buffer (Sigma) for five minutes, and the cells were repelleted for the same speed and time. Cells were then resuspended in 2% bovine serum albumin (BSA) (Sigma) + 1x PBS (2%BSA/PBS) and placed on ice until needed. For experiments determining the microglia to macrophage ratio in the brain, individual animals were assayed. Phenotypic analysis was performed using cells pooled from littermates.

3.7: Immunofluorescent Cell Staining

Cells were placed in every other well of a Costar 96 well cell culture plate (Corning) and centrifuged at 1500 rpm for 7 minutes at room temperature. Cells were blocked for at least five 5 minutes at room temperature in 0.25 μg of anti-mouse CD16/CD32 (Fcg III/II Receptor) (BD Pharmingen) diluted in 25 μl 2%BSA/PBS. 75 μl of the appropriately diluted antibody combination was added to each well and incubated for at least 20 minutes at 4^{o}C in the dark (for details, see Table 1). After incubation, cells were centrifuged and washed twice in 200 μl PBS+BSA. Cells were either assayed fresh or fixed in 2% paraformaldehyde/ PBS and kept at 4^{o}C until analysis.

For intracellular antigen staining, fixed cells were pelleted as mentioned previously and washed twice in PBS. Cells were resuspended in 200μl of 0.1% saponin/1xPBS and incubated at room temperature for between 10- 20 minutes to perforate the cell membrane. After washing in 0.1% saponin/PBS, samples were incubated with 50 μl of rat anti-CD68 (Serotec, Raleigh, NC) diluted in 0.1% saponin/ PBS and incubated at 4^{o}C for at least 20 minutes. After one wash, 50 μl of PE conjugated anti-rat IgG (Caltag) in 0.1% saponin/ PBS was added to the samples and incubated for 20 minutes at 4^{o}C. Cells were washed twice, resuspended in PBS and kept at 4^{o}C until analysis.

3.8: Flow Cytometry

Flow cytometric analysis was performed on a FACSAria or FACScan (BD Biosciences) using FACSDiva or Cell Quest Software (BD Bioscience). FlowJo (Treestar) software was used for post- acquisition analysis. In initial experiments, ViaProbe (BD Bioscience) staining was used to gate upon the live cells. Forward versus side scatter plots were used to exclude debris and doublet events. Microglia and macrophage populations were identified by their relative expression of CD45 and F4/80. The expression level of CD45 differs between microglia and macrophages which can be used distinguish between these two cell types[75,76]. Due to the common nature of CD45 expression on a number of various cell types, we used the specific macrophage/ microglia marker F4/80 to identify these cell types. For the purposes of this study, populations referred to as microglia are $CD45^{low}F4/80+$, and those referred to as macrophages are $CD45^{high}F4/80+$. In order to determine percent infected cells, EC and mock infected histograms of gp70 staining were overlayed and the point at which the graphs intersected was determined. And events falling above that point gated accordingly and considered positive. This gate was also used to determine positive cells in the microglia population. Percent above background was calculated by taking the average EC infected positive percentage and subtracting from the average mock infected positive percentage.

3.9: Histology and Immunohistochemistry

Tissues sections were processed and embedded in paraffin and 4 um slides cut at the Louisiana State University School of Veterinary Medicine Histology Laboratory. Slides were incubated at $56^{o}C$ overnight to adhere the tissue to the glass. Sections were incubated twice in xylenes for fifteen minutes to remove residual paraffin and rehydrated with five minute incubations in 100%, 95%, 70% ethanol, and twice in PBS. Antigen retrieval was performed

using sodium citrate antigen retrieval buffer in a decloaking chamber (Biocare Medical, Concord, CA) set at 120°C for 20 minutes and cooled to 90°C. Pressure consistently read between 12-15 psi. When slides reached 90°C, they were rinsed four times with ultra pure water by replacing half of the volume of antigen retrieval solution with water. Slides were then washed twice with 0.5% fish skin gelatin (Sigma)/ PBS (0.5% FSG/ PBS) for ten minutes on a rocker. To reduce potential nonspecific antibody binding due to extraneous protein-protein interactions, slides were incubated in a humidity chamber (Fisher, Hampton, NH) in 175 µl normal donkey serum blocking solution for at least 30 minutes. All incubations were done in a humidity chamber and slides were covered with parafilm coverslips. Parafilm coverslips were removed and excess blocking solution was tapped off. Slides were incubated overnight at 4°C with goat polyclonal anti-gp70 at 1:500 in 0.5% FSG/PBS. Slides were then tapped off to remove excess primary antibody and washed twice in 0.5% FSG/PBS for at least ten minutes each. A biotinylated rabbit anti goat secondary antibody (Molecular Probes) was applied at a dilution of 6.67µg/ ml in 0.5% FSG/PBS and each slide was covered with a parafilm coverslip and incubated for at least 30 minutes at room temperature. After incubating, slides were washed twice in 0.5% FSG/ 1x PBS. Streptavidin conjugated to AlexaFluor 594 (Molecular Probes) was used for detection at 4 µg/ ml diluted in 0.5% FSG/PBS and incubated for 30 minutes. Slides were washed twice in 0.5% FSG/ 1x PBS and reblocked in normal donkey serum blocking solution for at least thirty minutes. Polyclonal rabbit anti- Iba1 (Wako) was applied to the slides at 2.5 µg/ ml and either allowed to incubate at 4°C overnight or for at least 30 minutes at room temperature. Following two washes for at least 10 minutes in 0.5% FSG/PBS, an AlexaFluor 488 (Molecular Probes) goat anti-rabbit secondary antibody was applied at 6.67 µg/ ml and incubated at room temperature for at least 30 minutes. Slides were washed twice for at least 10

minutes in 0.5% FSG/PBS and counterstained with 100 ng/ ml DAPI (Molecular Probes) for up to 25 minutes and washed once in 0.5% FSG/PBS. Slides were mounted with ProLong Gold antifade reagent (Molecular Probes) and allowed to set for at least two hours at 4°C to allow for maximum effectiveness of the antifading properties.

3.10: RNA Processing for Real Time PCR

Isolation: Tissues were removed from storage at -80°C and placed in a precooled Tropi-Cooler set at -19°C and were homogenized in 2 ml Trizol (Invitrogen) in a sterile dounce homogenizer, pestle size B. The homogenate was split between 1.5 ml centrifuge tubes, and the homogenizer was rinsed with 1 ml Trizol with the wash discarded. Homogenates sat at room temperature for 5 minutes to allow for complete dissociation of nucleoprotein complexes, and 200 µl of chloroform was added to each tube. Tubes were vigorously agitated and incubated at room temperature for 2-3 minutes. Samples were centrifuged at 12,000 x g for 15 minutes at 4°C in an Eppendorf table-top centrifuge to separate the phases. The colorless aqueous phase containing the RNA was removed and placed in a new 1.5 ml centrifuge tube. RNA was precipitated using 600 µl of isopropanol and incubating the samples at room temperature for at least ten minutes. Samples were centrifuged at 12,000x g for 10 minutes at 4°C. The RNA formed a cloudy pellet at the bottom of the tube. Supernatants were poured off; 1 ml of 70% ethanol was added; samples were vortexed briefly to dislodge the pellet, and centrifuged at 7,500 x g for 5 min at 4°C. Ethanol was poured off; pellets were air dried for 5-10 minutes, and 50 µl of RNAse-free water was added to the pellets. After incubating at 55°C for 10 minutes on a dry heat block, samples were centrifuged briefly and stored at -80°C.

DNase Treatment: After Trizol purification, RNA was then DNAse treated to remove any residual genomic DNA from the purified RNA. A master mix was made from the Ambion

DNase I kit by combining 10 µl DNase buffer, 15 µl (30 units) of DNase I, and 70 µl RNase-free water for each sample to be treated. 95 µl of the master mix was added to a clean 1.5 ml centrifuge tube along with 10 µg of the appropriate RNA sample. Samples were mixed by pipetting up and down, centrifuged briefly, and incubated at 37°C for 30 minutes. RNA was removed using a Zymo RNA Clean-up Kit. 400 µl of RNA-Binding buffer was added to the sample and pipetted up and down to mix. Mixture was transferred to a Zymo-spin column and centrifuged for 30 seconds at full speed. RNA was washed twice with 350 µl of wash buffer and centrifuged at full speed for 30 seconds before eluting in 50 µl of RNase- free water. Samples were spun briefly and the eluate was stored at -80°C or used immediately for reverse transcription.

Reverse Transcription: A master mix was made using Bio- Rad's iScript cDNA Synthesis Kit containing 10 µl nuclease-free double distilled water, 4 µl of 5x iScript Reaction Mix, and 1 µl iScript reverse transcriptase (iScript RT) for each sample. An additional 1 µl of water was used in place of the iScript RT for the non-reverse transcribed (no-RT) controls. Approximately 1 µg of the appropriate RNA sample was added to 15 µl of master mix in a 0.5 ml tube 15 µl of this was dispensed to the bottom of a 0.5 ml centrifuge tube. Mixes of RNA were made and serially diluted 1:5, 1:25, and 1:125 to gauge the efficiency and sensitivity of the reverse transcription process. Tubes were placed in an MJ Research PTC Thermal Cycler and run under the following conditions: 25°C for 5 minutes, 42°C for 30 minutes, 85°C for 5 minutes, and 20°C forever. Upon finishing the program, samples were briefly centrifuged, 80 µl of nuclease free water was added to each, vortexed, and centrifuged. cDNA was stored at -20°C until use.

3.11: Real Time PCR

A master mix was made using iTaq SYBR Green Supermix with Rox containing 17.5 µl 2x iTaq SYBR Green Supermix with Rox, 1.75 µl of forward and reverse primers (1.8 µM final concentration) and 9 µl Rnase free H_2O for a total volume of 30 µl per sample. This was dispensed into one well of a 96 well PCR plate kept in a cooler block. 5 µl (10 ng) of cDNA or water was added to the appropriate well, the plate was covered with Rnase/ DNase free film, vortexed to mix and centrifuged at 1500 rpm for 5 minutes. Film was removed and samples were dispensed in triplicate into a 384 well plate (Applied Biosystems) using a Matrix electronic repeating pipette (Matrix Technologies) Plates were spun at 1500 rpm for 5 minutes and kept at 4^oC until analysis on an Applied Biosystems 7900 and acquired with SDS 2.2.2 (Applied Biosystems). Primers for real-time PCR analysis are were designed using Primer3 software. Specificity was confirmed by blasting the primer pairs against the National Center for Biotechnology Information (NCBI) website. Absence of genomic DNA contamination was seen by running reactions without reverse transcription. Non-reverse transcribed samples were either negative for all genes after 40 cycles or had at least 1,000 fold lower expression. Gene expression was quantified using the cycle number at which each sample reached a fixed fluorescence threshold (C_T). Data are presented as the percent difference in C_T value (log_2) of each sample subtracted from its *Gapdh* CT value ($\Delta C_T = C_T$ *Gapdh*-C_T gene of interest). This controls for variations in RNA concentrations between each sample. Primers are shown in Table 2.

3.12: Statistical Analysis

All statistical analysis was performed using GraphPad Prism software (San Diego, CA).

Table 2: Primers used in this study listed by gene.

Gapdh	Forward	TGCACCACCAACTGCTTAGC
	Reverse	TGGATGCAGGGATGATGTTC
Fb29gag	Forward	CCCGTGGCGGATTCTACT
	Reverse	TCGGAGAAAGAGGGGTTGTTA
F480	Forward	ACAAGTGTCTCCCTCGTGCT
	Reverse	AACATGGTGCTTTCCACAGTC
Gfap	Forward	CGTTTCTCCTTGTCTCGAATGAC
	Reverse	TCGCCCGTGTCTCCTTGA
Aif1	Forward	GCCTAAGACAACCAGCGTCT
	Reverse	GACGGCAGATCCTCATCATT
Cd68	Forward	ACCACCAGTCACGGAAATGT
	Reverse	CCAACAGTGGAGGATCTTGG
Cd80	Forward	CCTTGCCGTTACAACTCTCC
	Reverse	CAGGCCCAGGATGATAAGAG
Cd86	Forward	CTCCTCCTTGTGATGCTGCT
	Reverse	GCCTTCACTCTGCATTTGGT
Tnf	Forward	CCACCACGCTCTTCTGTCTAC
	Reverse	GAGGGTCTGGGCCATAGAA
Tnfsfr1a	Forward	GCTGACCCTCTGCTCTACGA
	Reverse	CCATCCACCACAGCATACAG
Tnfsfr1b	Forward	GCATCGTGAACGTCTGTAGC
	Reverse	GACGGACACTCCTCCTGAGA
Tradd	Forward	GGTGGAGCCATACAGGTAGC
	Reverse	AAGAGTCAGTGGCCGGTTC
Traf2	Forward	GGCTGTGGCAAGAAGAAGAT
	Reverse	TAGGGCTAGGTGTTCCCGTA
Tnfsfr6	Forward	GAATTACCCATGTCCCCAGA
	Reverse	CTCTAGGCCCACAAGATGGA
Fadd	Forward	GATGGATGGGATTGAGGAGA
	Reverse	CTCACAGATTCCTGGGCTTC

Chapter 4: Results

4.1: Microglia/Macrophage Related Genes Are Upregulated in the Brain During EC Virus Infection

Previous studies demonstrated an increase in *Tnfa* and *F480* mRNA expression in the brains of EC infected mice as compared to mock infected controls[5]. Additionally, analysis of microglia and macrophages by immunohistochemical staining show increased immunoreactivity when stained with a microglia/macrophage specific antibody (Iba1) in EC infected mice (Fig. 4). Iba1 and antibodies directed toward the virus envelope protein colocalized on the surface of the same cells (Fig. 4E, yellow color) indicating that microglia and macrophages are infected with EC.

To determine if EC infection altered the expression of TNFα receptors, or costimulatory molecules normally expressed on microglia/macrophages, we analyzed brain tissue from infected mice at 28 dpi, a time point at which clinical disease begins to develop. *Cd86* mRNA levels were significantly increased in the brain of EC infected mice when compared to mock infected controls with slight but not significant increases observed in *Cd80 and Cd68* mRNA (Fig 5) . mRNA for TNFα receptors *CD120a* (TNFR1, p55, *Tnfsfr1a*) and *CD120b* (TNFR2, p75, *Tnfsfr1b*) was also increased. This suggests that microglia and macrophages may upregulate these molecules in response to EC infection.

4.2: Cell Enrichments From TNF-/- Animals Yielded More Microglia Than Mock Infected Controls Early in Infection

To examine the expression of costimulatory molecules and TNFα receptors directly on microglia/macrophages, we enriched for these cell types with Percoll gradients and analyzed for cell surface expression by flow cytometry. The time points were chosen because the virus has

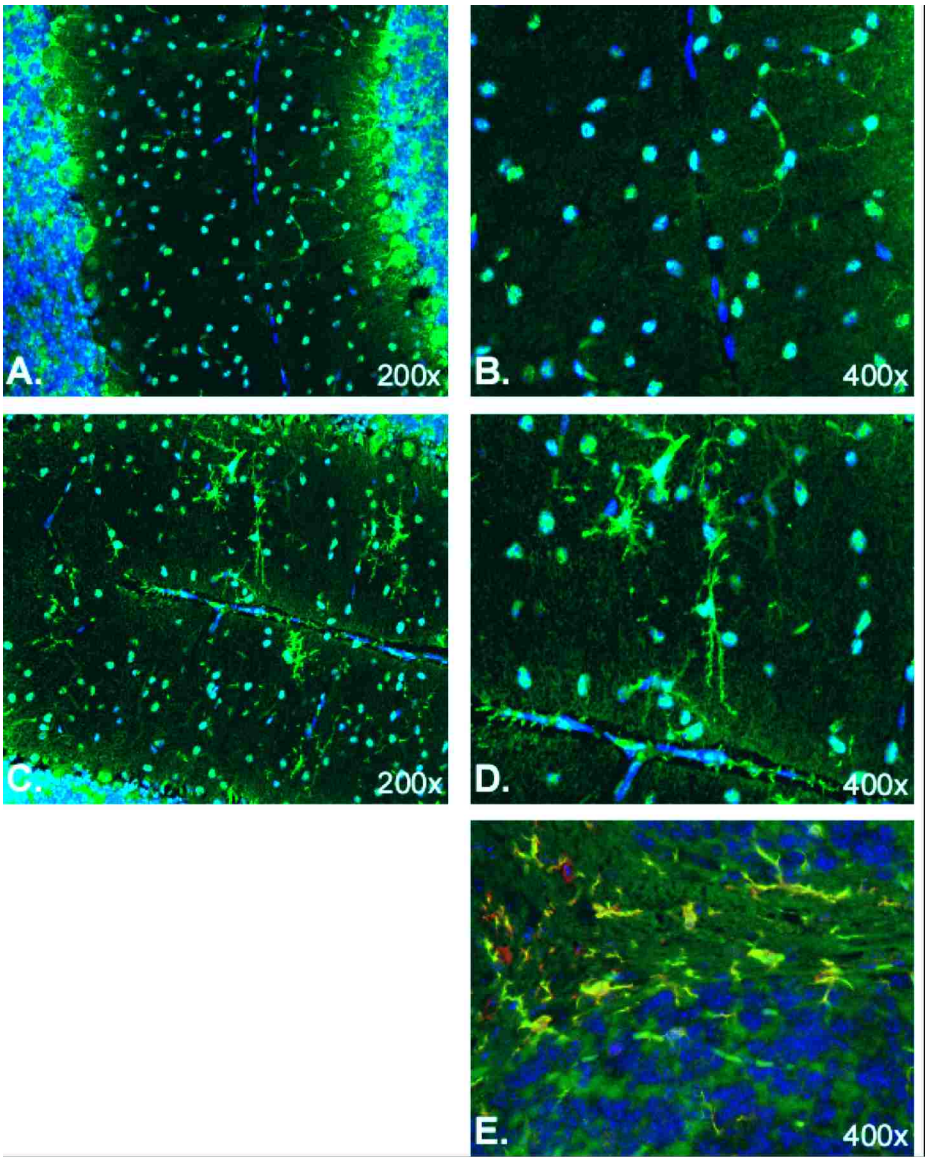

Figure 4: EC infected mice have a higher number of activated microglia/macrophages at 28 dpi. Animals were inoculated as described in the Materials and Methods. At 28 dpi, brains were removed and fixed for 48 hours in 3.7% neutral buffered formalin. Sections were cut and mounted on slides for immunohistochemical analysis. Antigens were retrieved using citrate target retrieval with a combination of temperature and heat in a decloaking chamber. Sections were stained with rabbit anti Iba-1 [48] with an AlexaFluor 488 secondary for green fluorescence. DAPI was used as a counterstain (blue fluorescence). Images were visualized with a Leica microscpope and captured with a digital camera. Cerebellum of a mock infected WT mouse at (A) 200x and (B) 400x. Cerebellum of an EC infected WT mouse at (C) 200x and (D) 400x. (E) Slides from an EC infected WT mouse at 28 dpi were also incubated with goat anti-gp70 with a biotinylated anti-goat secondary applied and visualized with streptavidin conjugated AlexaFluor 594 (400x). Dual labeling is seen as yellow.

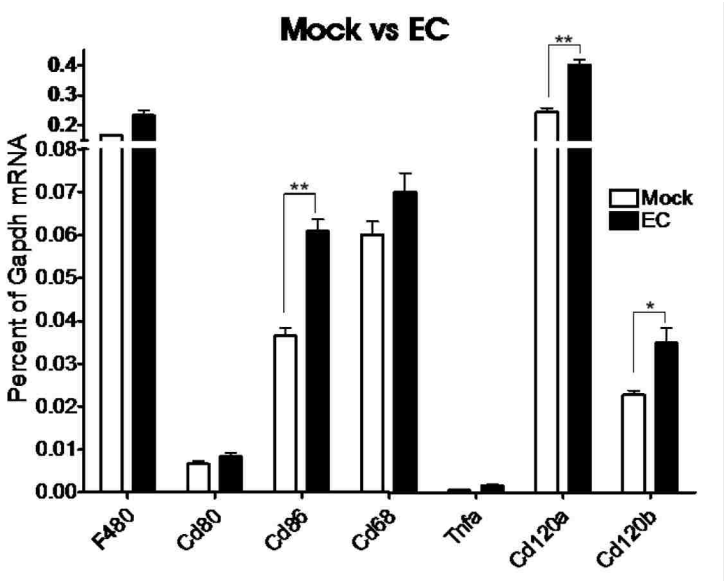

Figure 5: Genes upregulated during EC infection. Neonatal 129SvEv mice were inoculated with 10^4 FFU of EC within 24 hours of birth. At 28 dpi, brain tissue from mock (n=3) and EC (n=5) infected was removed with sagittal halves flash frozen for RNA isolation and cDNA production as described in the Materials and Methods. mRNA expression was determined using quantitative real time PCR with samples run in triplicate. Data are presented as the expression of the gene of interest as a % of *Gapdh* mRNA expression. Statistical analysis was done using a one-way ANOVA with the Neuman-Keuls post-test.

established the infection by 14 dpi, and WT animals begin to show symptoms of the neurological disease at 28 dpi. Microglia and macrophages were identified by their relative expression of CD45, F4/80, and CD11b[41,77]. In agreement with previously reported findings, microglia and macrophages in this study exhibited the typical staining pattern of $CD45^{high}$ F480+ CD11b+ macrophages and $CD45^{low}$ F480+ CD11b+ microglia[41,77]. For further analysis, samples were gated as described in the Materials and Methods and shown in Fig. 6. Cells from mock infected TNF-/- and WT mice expressed similar levels of CD45, F4/80 and CD11b at both time points analyzed. Surprisingly, EC virus infection had a negligible effect on the expression of these features at both time points. However, infection with EC did appear to raise the number of microglia enriched from the brain with the largest difference seen in TNF-/- mice at 14 dpi (Fig. 7) whereas the number of macrophages was consistent for each strain at both time points.

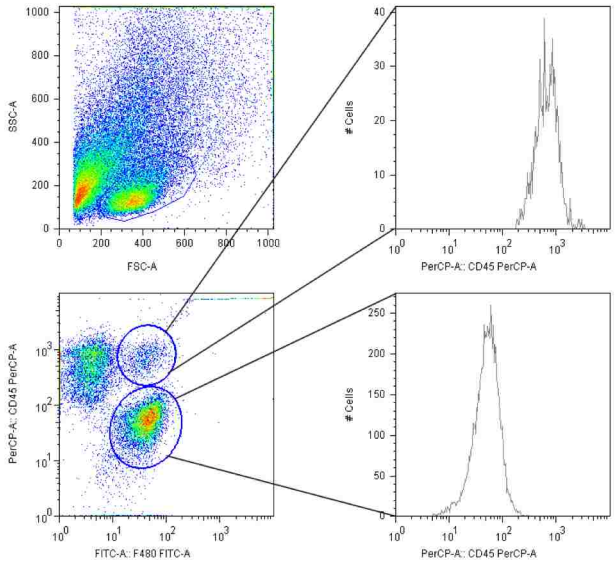

Figure 6: Separation microglia and macrophage populations by their relative expression of CD45. Microglia and macrophages were enriched from the brain tissue of a 28 dpi WT mouse using Percoll gradients and subsequently analyzed by flow cytometry. Cells were incubated with the proper dilution of directly conjugated primary antibody, washed, and fixed in paraformaldehyde before analysis. Cellular debris was gated out of the analysis based on previous ViaProbe staining for viable cells. The graph presented is representative of multiple experiments. Events falling within quadrant II were designated $CD45^{high}$ F4/80+and those falling within quadrant III as $CD45^{low}$ F4/80+. Macrophages exhibit a $CD45^{high}$ F4/80+ staining pattern whereas microglia are $CD45^{low}$ F4/80+. Similar gating criteria was used in all subsequent analyses.

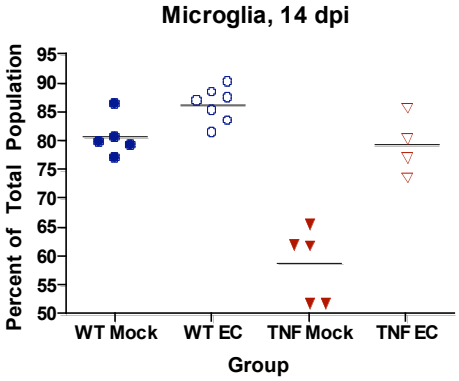

Figure 7: At 14 dpi, TNF-/- animals have a lower proportion of $CD45^{low}$ F480+ cells. Neonatal TNF-/- and wild-type control mice were infected with 10^4 FFU of EC within 24 hours of birth. Cells were enriched for and analyzed as described in the Materials and Methods. Data are presented as the percent of cells within the FSC vs. SSC gate that exhibit the F480+ $CD45^{low}$ staining pattern. Each symbol represents one animal. A siginificant decrease by a one way ANOVA with Neuman-Keuls post hoc tests was seen mock infected TNF-/- mice compared to the other groups ($P<0.001$), whereas there was no difference between or among the WT groups.

4.3: Macrophages and Not Microglia Are Predominantly Infected With EC

Both microglia and macrophages are potential targets of EC infection. Virus infection may influence activation and the subsequent release of potentially damaging factors. At both time points tested, microglia and macrophages enriched from WT and TNF-/- mice tested positive for the viral glycoprotein gp70 (Fig 8). At 14 dpi, 38% of macrophages enriched from EC infected WT mice were positive for virus as compared to 27% from EC infected TNF-/- mice. Surprisingly, virus was undetected in microglia enriched from either WT or TNF-/- mice (0.67% and 0.30% above background, respectively). At 28 dpi, 36% of from WT and 41% from TNF-/- mice were positive for virus, indicating similar levels of virus infected macrophages. A substantial increase in microglia infection was observed at 28 dpi, with 1.23% of WT and 5.01%

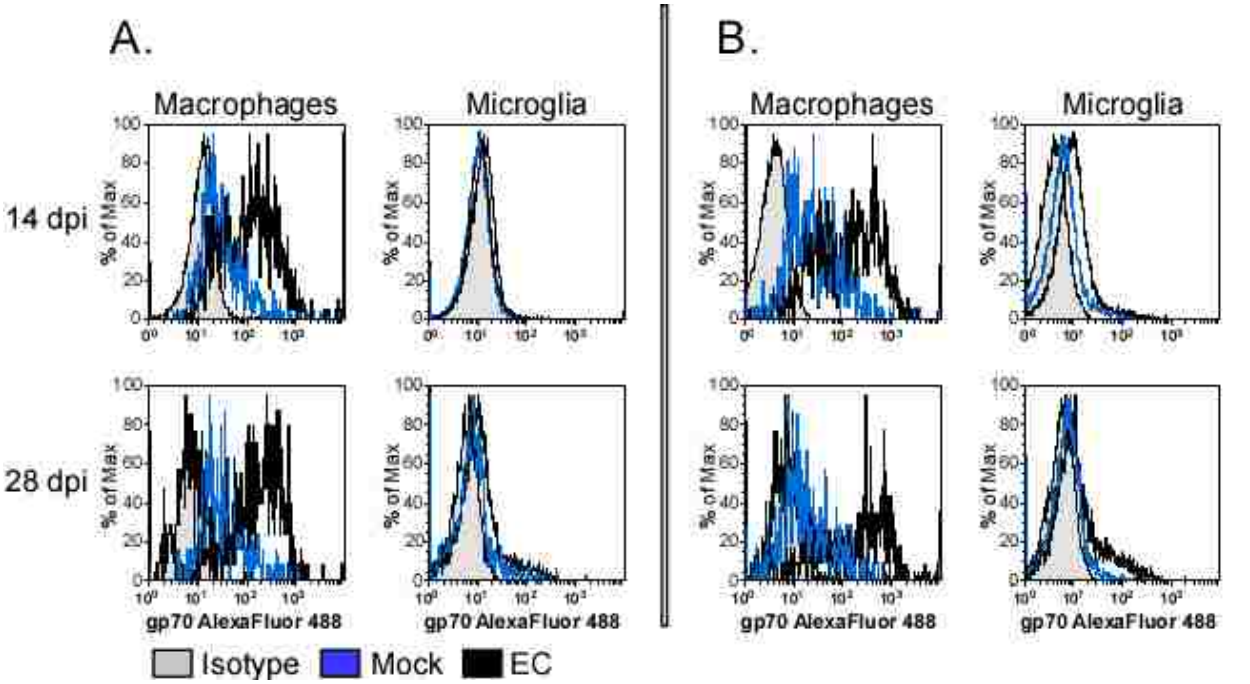

Figure 8: Macrophages were predominantly infected with EC early in infection, with more microglia staining for the virus protein by 28 dpi. Microglia and macrophages were enriched and analyzed from (A) WT and (B) TNF-/- mock and EC infected brains as described in figure 7. Cells were incubated in a polyclonal goat anti- gp70 primary antibody followed by rabbit anti-goat AlexaFluor 488 (Molecular Probes) to visualize the staining.

of TNF-/- microglia cells positive for the virus. This suggests that the virus infection starts in the macrophage population of the brain and it slowly spreads to microglia, indicating that macrophages more than microglia may serve as a reservoir for further virus infection in the brain.

4.4: Expression of Activation Features During EC Infection

Activation of microglia and macrophages has been associated with both neuroprotection and neuropathogenesis[5,78,79]. Previous studies indicate a potential role for TNFα in the activation of microglia/macrophages[5,32,33,78,79]. To determine if systemic TNFα deficiency has a detectable effect on the activation of these cell types during EC infection, we analyzed the expression CD68, CD80 and CD86 which are often upregulated on macrophages/ microglia following activation[78,80]. At both time points tested, markers were present and expressed at similar levels on microglia and macrophages enriched from mock infected WT and TNF-/- mice, with a slightly higher level of expression of CD86 on macrophages than microglia (Fig. 9, 14 dpi; Fig. 10, 28 dpi). No difference in the geometric means or mean channel numbers was observed between WT and TNF infected mice (Tbl. 3, 4). Expression of CD68, CD80 and CD86 was unchanged in TNF-/- or WT mice following EC infection at 28 dpi (Fig. 10), indicating that EC virus infection may not induce significant upregulation of these molecules.

4.5: TNFα Receptor Expression on Microglia/Macrophages

TNFα signaling has various outcomes depending on which of its two receptors it activates. Signaling through CD120a is associated with the proteotypic inflammatory responses and is usually initiated by secreted TNFα (rev. in [19]). The results of CD120b signaling tend to be tissue specific due its affinity for membrane bound TNFα(rev. in [19]). Microglia and macrophages expressed both TNFα receptors at each time point tested (Fig. 9, 14 dpi; Fig. 10, 28

Table 3: Average geometric means for the phenotypic features of macrophages and microglia that were analyzed by flow cytometry. Cells were enriched and analyzed as described in Figure 5. Antigen specific geometric means from the total macrophage or total microglia population were determined by FlowJo Software. Data from at least two separate experiments were used in the calculations. (a) mean, (b) range.

Strain	Inoculation	DPI	Cell Type	Value	CD11b	CD68	CD80	CD86	CD120a	CD120b
WT	Mock	14	Macrophage	GM	1027 ± 298.0	500 ± 139.0	64.7 ± 7.4	46.6 ± 14.5	6.7 ± 0.9	39.8 ± 20.2
WT	EC	14	Macrophage	GM	824 ± 244.0	573 ± 224.0	66.7 ± 12.6	46.5 ± 15.2	6.8 ± 1.0	35.8 ± 16.4
TNF	Mock	14	Macrophage	GM	1,185 ± 258.0	434 ± 33.0	115.0 ± 19.2	89.1 ± 2.4	7.5 ± 1.3	39.8 ± 4.3
TNF	EC	14	Macrophage	GM	861 ± 17.8	418 ± 35.0	122.0 ± 42.1	114.0 ± 22.4	7.1 ± 1.1	39.6 ± 4.9
WT	Mock	14	Microglia	GM	253 ± 29.0	200 ± 39.0	10.9 ± 2.1	28.7 ± 3.5	5.1 ± 0.3	25.8 ± 13.5
WT	EC	14	Microglia	GM	239 ± 47.0	188 ± 54.0	10.5 ± 2.7	28.7 ± 3.8	5.0 ± 0.3	25.2 ± 12.4
TNF	Mock	14	Microglia	GM	310 ± 48.0	204 ± 11.0	9.1 ± 0.7	31.3 ± 1.4	5.0 ± 0.3	19.7 ± 1.1
TNF	EC	14	Microglia	GM	290 ± 11.0	190 ± 40.0	9.4 ± 0.3	31.4 ± 1.8	4.8 ± 0.1	21.4 ± 9.6
WT	Mock	28	Macrophage	GM	1,445 ± 234.0	1276 ± 655.0	30.1 ± 2.2	22.3 ± 0.8	7.7 ± 0.2	22.1 ± 2.2
WT	EC	28	Macrophage	GM	1,007 ± 192.0	1457 ± 429.0	33.1 ± 1.9	26.3 ± 4.3	6.8 ± 1.4	23.5 ± 3.9
TNF	Mock	28	Macrophage	GM	311 ± 29.0	381 ± 44.0	32.4 ± 3.4	30.4 ± 0.9	8.8 ± 1.2	18.5 ± 1.5
TNF	EC	28	Macrophage	GM	495 ± 73.0	265 ± 3.0	35.1 ± 5.4	37.1 ± 1.1	11.3 ± 0.1	27.4 ± 1.7
WT	Mock	28	Microglia	GM	399 ± 18.0	157 ± 63.1	13.6 ± 8.3	22.2 ± 174.7	7.7 ± 3.3	7.7 ± 0.3
WT	EC	28	Microglia	GM	394 ± 21.0	163 ± 33.7	12.9 ± 6.3	22.5 ± 190.2	7.3 ± 23.6	7.3 ± 18.3
TNF	Mock	28	Microglia	GM	313 ± 11.0	197 ± 11.3	13.1 ± 11.8	23.5 ± 3.1	8.1 ± 14.7	8.1 ± 8.9
TNF	EC	28	Microglia	GM	336 ± 24.0	140 ± 1.2	12.6 ± 17.3	26.8 ± 29.8	8.6 ± 1.2	8.6 ± 6.8

Table 4: Average mean channel numbers for the phenotypic features of macrophages and microglia that were analyzed by flow cytometry. Cells were enriched and analyzed as described in Figure 5. Antigen specific mean channel numbers from the total macrophage or total microglia population were determined by FlowJo Software. Data from at least two separate experiments were used in the calculations. (a) mean, (b) range.

Strain	Inoculation	DPI	Cell Type	Value	CD11b	CD68	CD80	CD86	CD120a	CD120b
WT	Mock	14	Macrophage	MCN	253 ± 25.1	687 ± 31.9	463 ± 12.9	408 ± 39.1	211 ± 16.0	396 ± 68.9
WT	EC	14	Macrophage	MCN	240 ± 47.3	598 ± 45.9	466 ± 21.5	420 ± 38.0	212 ± 16.3	390 ± 51.1
TNF	Mock	14	Macrophage	MCN	310 ± 48.1	675 ± 8.6	536 ± 8.6	499 ± 3.2	223 ± 19.2	409 ± 12.0
TNF	EC	14	Macrophage	MCN	290 ± 11.7	707 ± 46.2	585 ± 95.5	544 ± 23.6	390 ± 156.9	311 ± 111.2
WT	Mock	14	Microglia	MCN	615 ± 13.3	532 ± 22.7	398 ± 103.0	407 ± 39.1	197 ± 24.8	384 ± 51.9
WT	EC	14	Microglia	MCN	606 ± 21.1	531 ± 20.2	398 ± 123.0	420 ± 38.0	190 ± 5.3	378 ± 33.9
TNF	Mock	14	Microglia	MCN	651 ± 38.8	575 ± 8.6	391 ± 1534.0	499 ± 3.3	202 ± 23.5	409 ± 12.0
TNF	EC	14	Microglia	MCN	631 ± 4.5	553 ± 96.0	463 ± 217.0	545 ± 22.0	408 ± 22.1	275 ± 99.8
WT	Mock	28	Macrophage	MCN	807 ± 18.2	778 ± 63.0	378 ± 8.3	342 ± 174.7	228 ± 3.3	343 ± 0.3
WT	EC	28	Macrophage	MCN	767 ± 21.4	805 ± 33.7	389 ± 6.3	382 ± 190.1	212 ± 23.6	350 ± 18.3
TNF	Mock	28	Macrophage	MCN	638 ± 10.8	558 ± 11.3	386 ± 11.8	379 ± 3.1	240 ± 14.7	324 ± 8.9
TNF	EC	28	Macrophage	MCN	964 ± 24.3	520 ± 1.2	394 ± 17.3	435 ± 29.8	270 ± 1.2	367 ± 6.8
WT	Mock	28	Microglia	MCN	666 ± 4.4	562 ± 12.6	285 ± 9.3	344 ± 12.7	227 ± 4.1	299 ± 10.1
WT	EC	28	Microglia	MCN	664 ± 10.9	566 ± 5.6	284 ± 4.3	357 ± 22.5	221 ± 4.2	278 ± 8.7
TNF	Mock	28	Microglia	MCN	642 ± 12.3	587 ± 10.8	286 ± 3.3	314 ± 56.2	231 ± 8.0	306 ± 3.1
TNF	EC	28	Microglia	MCN	336 ± 78.9	577 ± 41.9	282 ± 3.6	361 ± 9.3	240 ± 2.0	293 ± 10.9

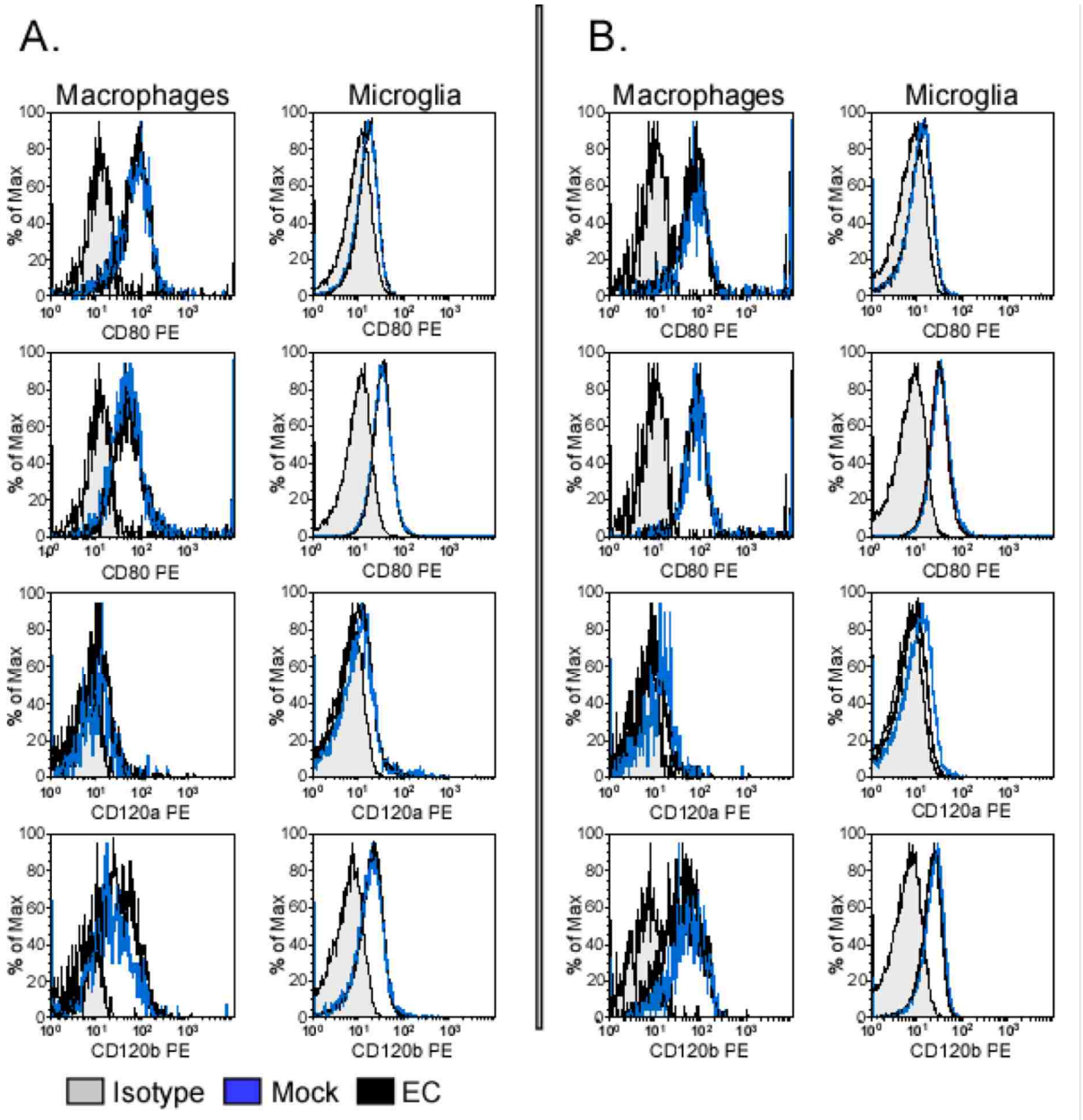

Figure 9: Microglia and macrophages enriched from mock and EC infected WT (A) and TNF-/- (B) mice at 14 dpi have similar expression of the markers CD80, CD86, CD120a, and CD120b. Microglia/macrophages from the brains of mice were enriched via Percoll gradients with the microglia/macrophage fraction residing between the 70% Percoll layer and the 37% isotonic Percoll layer. The residual brain tissue was removed before the microglia enriched fraction was harvested. The microglia/macrophages were then stained for cell surface markers to determine the purity of the fraction and for phenotypic analysis as described in figure 5. Data was collected on a FACSAria and analyzed with FlowJo software.

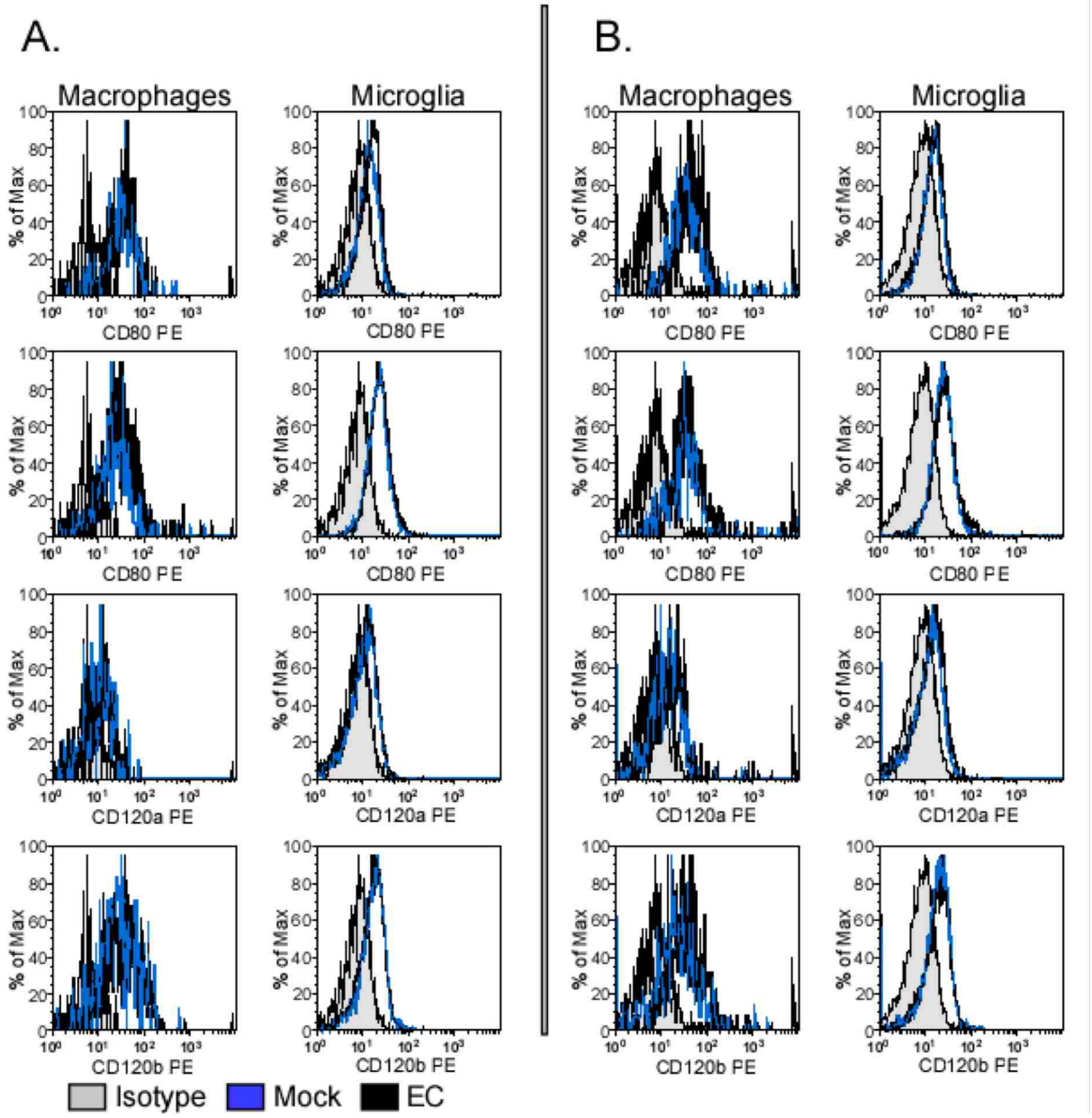

Figure 10: Expression of activation markers and TNF receptors at 28 dpi on macrophages and microglia was similar to that seen at 14 dpi. Microglia and macrophages were enriched and analyzed from (A) WT and (B) TNF-/- mock and EC infected brains as described in Figure 9.

dpi). Interestingly, neither the absence of TNFα or EC infection altered their expression on these cell types.

4.6: Minocycline Treatment Had No Effect on Delaying the Onset of Neurological Disease.

EC infection is known to induce *Tnfa* mRNA production and microglia/macrophage activation as measured by mRNA expression of *F480*[72]. To determine if inhibiting TNFα production and microglia/ macropage activation during an established viral infection would impede the development of neurological disease, we treated mice with minocycline which has the ability to decrease microglia/macrophage activation and TNFα[2]. Treatment was initiated at 14 dpi using a previously described concentration[81]. This will allow the virus an opportunity to establish a productive infection in the brain prior to treatment. Surprisingly, there was no statistical difference in survival curve analysis between the EC infected placebo and minocycline treated groups (Fig. 11), indicating that minocycline could not prevent EC induced disease.

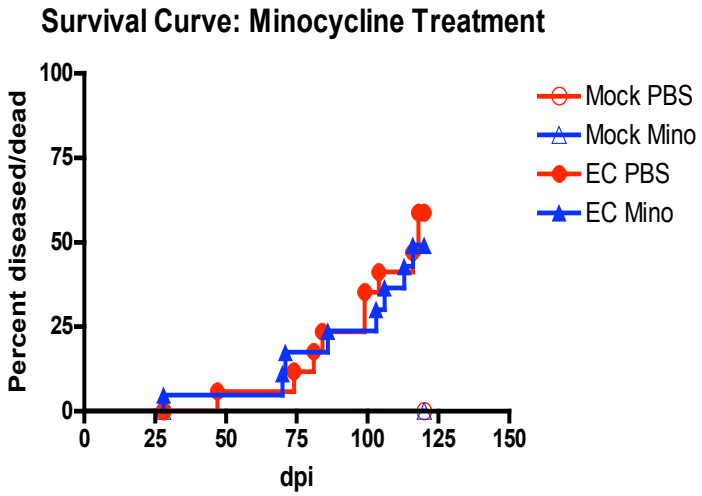

Figure 11: Administration of minocycline does not alter EC mediated disease. Mice were infected as described in figure 2. At 14 dpi, litters were randomly assigned a treatment regimen that consisted of one ip injection of 25 µl phosphate buffered saline (PBS) or 35 mg/kg minocycline in 25 µl PBS every other day. Animals were observed daily for obvious signs of neurological disease characterized by ataxia, hind limb paralysis or seizures. Data are presented as percent of mice exhibiting severe neurological disease for 16 Mock PBS, 20 Mock minocycline, 22 EC PBS and 21 EC minocycline mice. Statistical analysis was performed with a Kaplan-Meier survival test using GraphPad Prism.

4.7: Effect of Minocycline Treatment on Virus Levels, Microglia/Macrophage and Astrocyte Activation.

Despite the lack of an influence on neurological disease, minocycline treatment may influence viral replication, microglia/macrophage activation and/ or TNFα production[2,31]. At 28 dpi, brain tissue was removed for quantitative real time PCR analysis of mRNA expression. We examined mRNA expression of genes that are upregulated during EC induced neurological disease to determine of minocycline treatment had an effect on their mRNA expression. Surprisingly, minocycline treatment did not alter the mRNA expression of microglia/macrophage markers *F480* or *Aif1* (Fig. 12B, 13A). There was a slight, but not statistically significant, decrease in both *Fb29gag* and *Gfap* (Fig. 12A, C) indicating that treatment may have slightly reduced viral load and astrocyte activation during EC infection.

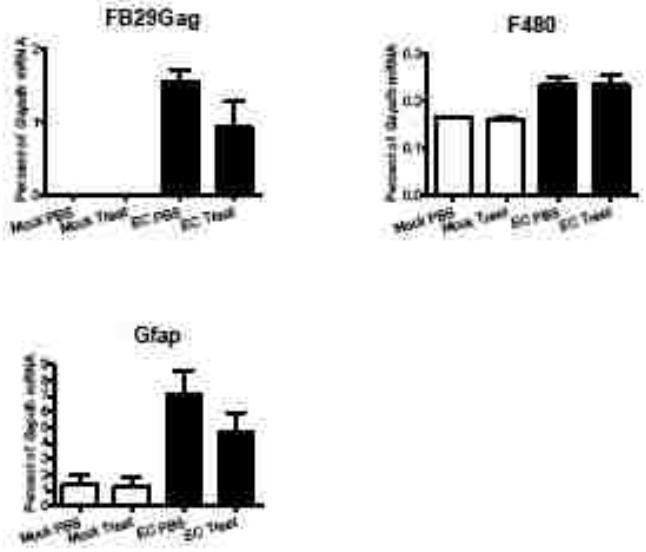

Figure 12: Genes corresponding to virus load and astrocyte activation were slightly decreased in the EC infected minocycline treated animals. Brain tissue was removed from PBS and minocycline treated mock and EC infected animals at 28 dpi and processed for real-time PCR as described in the Materials and Methods. Data are presented as the expression of the gene of interest as a percent of *Gapdh* mRNA expression. Statistical analysis was done using a one-way ANOVA with the Neuman-Keuls post-test. For mock infected PBS and minocycline treated groups n=3, and both EC infected groups had an n=5. All groups are composed of animals from multiple litters.

mRNA expression of *Aif1, Cd80, Cd86,* and *Cd86* were not altered by minocycline (Fig. 13). Thus, minocycline did not substantially influence mRNA expression of microglia/macrophage activation molecules or those associated with EC virus infection

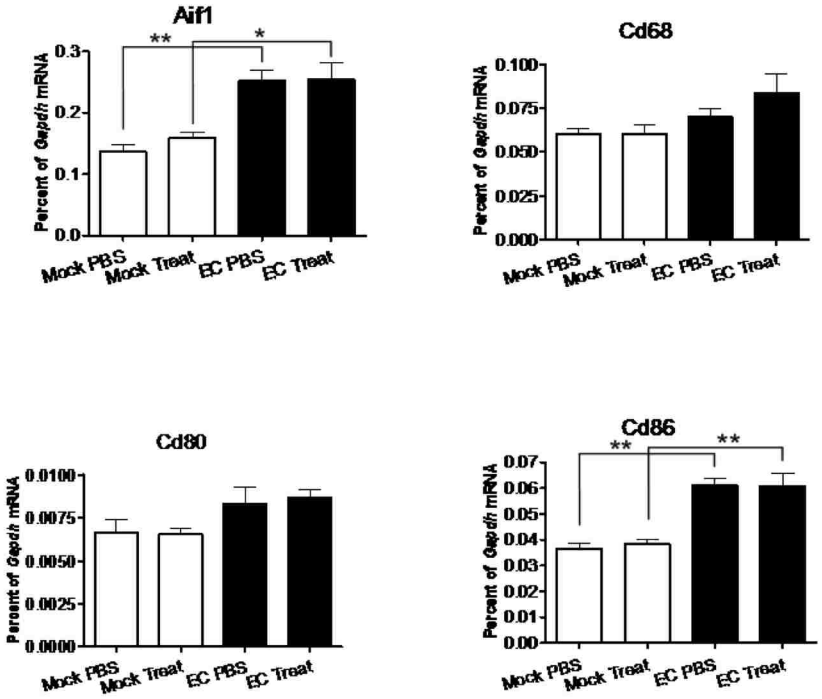

Figure 13: EC infection correlates with the increase in microglia activation genes *Aif1* (A) and *Cd86* (D). Samples were collected and processed as mentioned in Figure 11. The genes are as follows: *Aif1* (A), *Cd68* (B), *Cd80* (C), and *Cd86* (D). Statistical analysis was performed using a one-way ANOVA with the Neuman-Keuls post-test. For mock infected PBS and minocycline treated groups n=3, and both EC infected groups had an n=5. All groups are composed of animals from multiple litters. Where indicated, * denotes $p<0.05$ and ** denotes $p<0.01$.

4.8: Minocycline Treatment Influences mRNA Involved in Signaling Within the TNF Superfamily

In addition to decreasing microglia/macrophage activation, minocycline treatment is associated with decreased TNFα expression[2]. EC infection did increase *Tnfa* mRNA in PBS and minocycline treated groups and that minocycline reduced *Tnfa* mRNA in EC infected mice albeit at a statistically insignificant level (Fig. 14A). This agrees with previous studies showing *Tnfa* mRNA upregulation only in localized areas of the brain following EC infection[5]. To determine

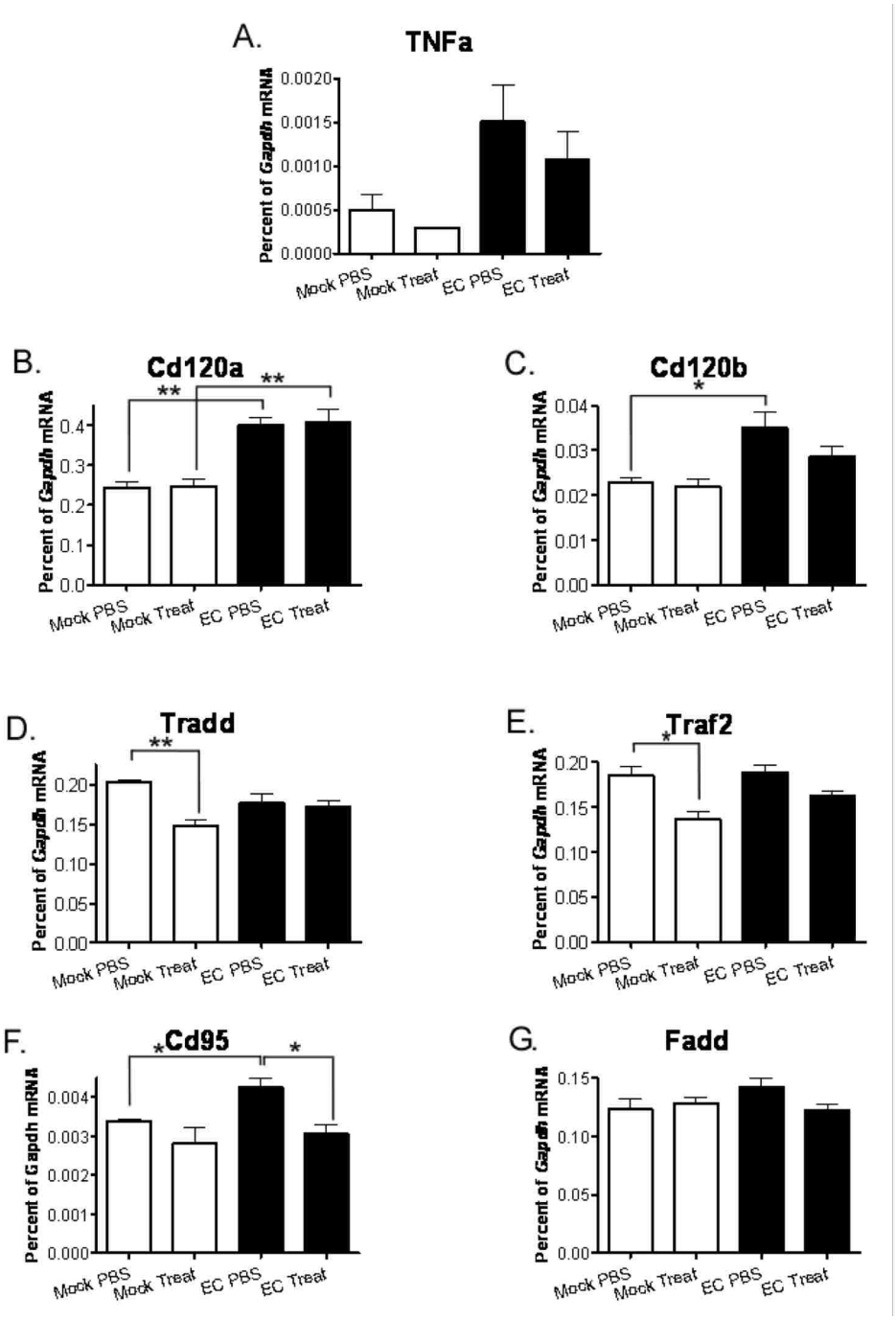

Figure 14: Expression of *Tnfa* (A) *Tnfsfr1a* (B), *Tnfsfr1b* (C), *Traf2* (D), *Tradd* (E), C*d95* (F), and *Fadd* (G) during minocycline treatment. Brain tissue was removed from PBS and minocycline treated mock and EC infected animals at 28 dpi and processed for real-time PCR as described in the Materials and Methods. Data are presented as the expression of the gene of interest as a percent of *Gapdh* mRNA expression. Statistical analysis was performed using a one-way ANOVA with the Neuman-Keuls post-test. For mock infected PBS and minocycline treated groups n=3, and both EC infected groups had an n=5. All groups are composed of animals from at least two litters. Where indicated, * denotes $p<0.05$ and ** denotes $p<0.01$.

if minocycline treatment had an effect on genes involved with signaling, we analyzed the mRNA levels for receptors and adaptor molecules within this family. Treatment with minocycline significantly lowered the basal level expression of *Traf2, Tradd*, and *Cd95* (Fig. 14D, E, F). EC infection in PBS treated animals led to an increase in *Cd120a, Cd120b*, *Traf2*, *Cd95*, and *Fadd* (Fig. 14B, C, E, F, G). Interestingly, minocycline treatment during EC infection reduced the expression of *CD120b*, *Traf2, Cd95,* and *Fadd* (Fig. 14C, E, F, G). The finding of decreased *Tradd* and *Traf2* mRNA may be important in understanding how minocycline may potentially influence the TNF signaling cascade through the expression of accessory molecules or receptor expression.

Chapter 5: Discussion

In the current study, we analyzed the influence of TNFα on the activation phenotype of microglia and macrophages and the expression of genes associated with TNFα signaling and microglia/macrophage activation in animals treated with minocycline during EC infection. Activation features were present and expressed at similar levels on microglia and macrophages enriched from mock infected WT and TNF-/- animals, with a higher level of expression of CD86 on macrophages. These markers were unchanged on microglia or macrophages by EC infection in both WT or TNF-/- mice. Thus, neither systemic absence of TNFα or EC infection dramatically altered the phenotypic profiles of these cells. Administration of minocycline to inhibit microglia/macrophage activation had no statistically significant effect on delaying the onset of neurological disease during EC infection. However, minocycline may alter the course of TNFα signaling as it interferes with mRNA expression of TNFα receptors and signaling molecules, this therefore may inhibit signal transduction.

Real time PCR analysis at 28 dpi showed an increase in *Cd80, Cd86, Cd120a* and *Cd120b* mRNA from the whole brain indicating an upregulation of costimulatory molecules and TNF receptors in EC infected mice (Fig. 5). Microglia and macrophages enriched from mock infected WT and TNF mice did test positive for these markers, but there was no detectable increase in expression in response to EC infection on the surface of these cells (Fig. 9, 10). It is possible that a subset of highly activated macrophages and microglia with increased expression of these markers did not survive the enrichment process. Alternately, another cell type may be responsible for the elevated levels of mRNA of these markers observed in EC infected mice. For example, dendritic cells may be recruited to the brain, become activated in response to EC infection and upregulate expression of CD80 and CD86[82]. Reactive astrocytes also have been

shown to express these molecules on their cell surface and could contribute to the elevated levels of *Cd80* and *Cd86* mRNA[83].

The disparities between the upregulation of genes by real-time PCR but not by flow cytometric analysis may be attributed to differences with the technique. It is possible that the mRNA increase observed at 28 dpi precedes protein expression on the surface of the cell, thereby explaining the discrepancies between the flow and real- time PCR data. Real- time PCR analysis can detect small alterations in gene expression with high fidelity can be significant due to its sensitivity and reproducibility whereas flow cytometric analysis lacked the ability to do so. One of the limitations of real- time PCR analysis of a total tissue is that gene expression from a specific cell population cannot be identified. Once a gene of interest has been identified, then *in situ* hybridization could be a potential next step to determine the cell type and location in the brain where the gene is expressed. Alternately, mRNA from FACS sorted microglia and macrophages could be purified for gene analysis of activation features. The result could then be directly compared to the surface expression of the molecule to determine if RNA expression in that very specific cell population correlated with the protein expression.

A current theory in regards to HIV-1 associated dementia suggests that increased trafficking into the brain of infected monocytes late in the course of infection may be the first step in clinical HAD[84]. A similar situation may be occurring during EC infection, where EC appears to infect macrophages in the brain prior to detectable microglia infection at 28 dpi. Histolgical examination of tissues dual-stained for Iba1, a microglia/macrophage marker, and gp70, a virus envelope protein, indicates that the virus infected cells were in brain tissue rather than in circulation (Fig. 4). In the early stages of EC infection, infected monocytes may migrate to the brain where the virus infection spreads among resident macrophages and microglia. It is

also possible that the endothelial cells lining the blood vessels in the brain become infected first. The virus may then spread to perivascular macrophages and then to nearby microglia. The increase in microglia numbers enriched from EC infected TNF-/- mice (Fig. 7) suggests that this population may be expanding possibly in response to the viral insult. This rapid increase in cell number may explain the increase in infection rate seen in the microglia population for retroviruses utilize machinery from an actively dividing cell in order to replicate[85].

TNF-/- mice grow and develop as a normal WT mouse, but these animals lack follicular dendritic cell networks and germinal centers that are important for B cell development[86]. It is unlikely that the lack of germinal centers could contribute to the reduced number of infected macrophages in the brain of TNF-/- mice, but it is possible that the absence of follicular dendritic cell networks could potentially slow the spread of the viral infection to macrophages in the peritoneum. In addition, another possible explanation for the large number of infected macrophages versus microglia in the brain could be due to receptor expression. Polytropic retroviruses utilize XPR-1 to mediate entry into the cell, and it could be that macrophages express the receptor at a higher level making them potentially more susceptible to infection.

Minocycline's beneficial influence upon neuroinflammation has been shown in multiple models of neurological disease including reovirus infections, Huntington's disease, Alzheimer's disease, and SIV[58,60,61,63,81]. Mincycline treatment is often associated with decreased microglial activation and TNF secretionα[2,65,66,81,82]. In the current study, minocycline did not confer any benefit in terms of delaying the onset or decreasing the incidence of neurological disease (Fig. 11). It is possible that a higher dose could have possibly had an effect on the onset of EC induced neurological disease. However, the dosage used in this study has been successfully used to observe differences in the onset of neurological disease in viral induced encaphilitis[81] when

given concurrently with infection. Additionally, a single treatment of minocycline has been effective in decreasing microglial activation[87]. Previous studies with minocycline are usually undertaken in an adult animal model of disease, whereas this model utilizes neonatal infection. Treatment of neonatal mice with minocycline is lethal (unpublished observation), so administering the first treatment either prior to or concurrently with infection is not possible in this model. Also, infection cannot be delayed due to the fact that mice need to be inoculated with the virus within one day of birth for optimal disease development[88]. It may be that minocycline treatment is ineffective in already established or slowly progressing viral diseases. This could be to the slow rate at which the virus spreads to the brain, or that the virus has already initiated the chain of events that induces pathogenesis. It would be of interest to determine if minocycline treatment could delay disease in another retrovirus model that does not require neonatal inoculation, so that the system could be primed by a pretreatment with minocyline or administered at the time of infection.

Decreased microglial activation during minocycline treatment has been measured by different methods including decreased proliferation during treatment, or decreased IL-1β or TNFα secretion[2,63,65,81]. However, analysis of genes associated with microglia and macrophage activation had yet to be performed. Minocycline had no effect on decreasing mRNA expression of *F480, Aif1, Cd80, Cd86, Cd120a or Cd120b* (Fig. 12B, 13A, 13C, 13D, 14B, 14C) in the brains of mock infected mice but we did find decreased expression of *Tradd* and *Traf2* in both the mock and EC infected treated groups. The finding of decreased mRNA *Tradd* and *Traf2* mRNA may be important in understanding how minocycline could influence the TNF signaling cascade not only in this model but also for other models that may utilize this drug to inhibit TNFα.

The ability of minocycline to decrease TNFα secretion in microglia cultures *in vitro* has been well established[2,64], but the question remains as to how this influences the bigger picture of TNF signaling *in vivo*. TRAF2 interacts with death and non-death domain containing receptors of the TNF Superfamily: CD120a and CD95 (death) and CD120b (non-death). Due to its lack of a death receptor, CD120b can bind directly to members of the TRAF family whereas CD120a involves TRAF2 indirectly through interacting with TRADD which will bind to TRAF2 (reviewed in [89]). The subsequent signaling cascade induced by TRAF2 recruitment is regulated by molecules that to interfere with the process by blocking protein interactions or modifying the composition of the complexes[25]. TRADD mediated signaling usually results in apoptosis, whereas signaling through TRAF2 is often associated with cell survival. Under normal circumstances, inhibiting TRAF2 may potentially be detrimental to the host for this protein often mediates anti-apoptotic events[25,90]. During HIV infection, one of the downstream effects of TRAF2 mediated signaling is the activation of viral genome transcription[91]. Minocycline could possibly reduce HIV transcription by decreasing the level of Traf2 mRNA in the host cell, but this could inadvertently push non-target cells to signal through TRADD and predispose them to apoptosis. Although it is possible that through minocycline's ability to inhibit both *Traf2* and *Tradd* mRNA expression that the negative effects of reducing either of these alone may be negated.

In addition to potentially modulating TNFα signaling, minocycline treatment may have an additional and as yet recognized role in downregulating *Cd95* mRNA expression in the brain. Mock infected minocycline treated mice showed a significant decrease in *Cd95* mRNA expression as compared to their PBS treated controls (Fig. 14F). EC infection did increase expression of this gene in minocycline treated groups but not to the extent observed in the EC

infected PBS treated group. *Fadd* expression was also decreased in EC infected minocycline treated animals (Fig. 14G) suggesting the drug may influence downstream signaling further. The CD95- CD95L system has been associated with a variety of neurological diseases including both human and murine retrovirus infections of the CNS[27,28]. In addition to this, it is interesting to speculate upon how specifically inhibiting both *Fadd* and *Tradd* mRNA expression could influence a cell. By significantly reducing their expression, it may be possible to potentially force a cell to be insensitive to apoptosis and promote cell survival. Understanding how to better modulate the CD95- CD95L pathway and TNF induced apoptosis may lead to the ability to inhibit apoptosis and decrease neuronal cell loss and potentially delay disease onset. In doing so, this could decrease the severity of neurological disease in not solely this model but others in which this pathway has been directly linked to pathogenesis such as in experimental autoimmune encephalitis or Parkinson's disease[92,93].

References

1. **Johnson, R. T., J. D. Glass, J. C. McArthur, and B. W. Chesebro**. 1996. Quantitation of human immunodeficiency virus in brains of demented and nondemented patients with acquired immunodeficiency syndrome. Ann. Neurol. **39**:392-395.

2. **Giuliani, F., W. Hader, and V. W. Yong**. 2005. Minocycline attenuates T cell and microglia activity to impair cytokine production in T cell-microglia interaction. J. Leukoc. Biol. **78**:135-143.

3. **Sippy, B. D., F. M. Hofman, D. Wallach, and D. R. Hinton**. 1995. Increased expression of tumor necrosis factor-alpha receptors in the brains of patients with AIDS. J. Acquir. Immune. Defic. Syndr. Hum. Retrovirol. **10**:511-521.

4. **Wesselingh, S. L. and J. D. Glass**. 2000. Localization of HIV-1 DNA and tumor necrosis factor-alpha mRNA in human brain using polymerase chain reaction in situ hybridization and immunocytochemistry. Methods Mol. Biol. **123**:323-337.

5. **Peterson, K. E., S. Hughes, D. E. Dimcheff, K. Wehrly, and B. Chesebro**. 2004. Separate sequences in a murine retroviral envelope protein mediate neuropathogenesis by complementary mechanisms with differing requirements for tumor necrosis factor alpha. J. Virol. **78**:13104-13112.

6. **Esen, N. and T. Kielian**. 2006. Central role for MyD88 in the responses of microglia to pathogen-associated molecular patterns. J. Immunol. **176**:6802-6811.

7. **Nakamichi, K., M. Saiki, M. Sawada, Y. Yamamuro, K. Morimoto, and I. Kurane**. 2005. Double-stranded RNA stimulates chemokine expression in microglia through vacuolar pH-dependent activation of intracellular signaling pathways. J. Neurochem. **95**:273-283.

8. **Xiang, W., O. Windl, G. Wunsch, M. Dugas, A. Kohlmann, N. Dierkes, I. M. Westner, and H. A. Kretzschmar**. 2004. Identification of differentially expressed genes in scrapie-infected mouse brains by using global gene expression technology. J. Virol. **78**:11051-11060.

9. **Merlos-Suarez, A., J. Fernandez-Larrea, P. Reddy, J. Baselga, and J. Arribas**. 1998. Pro-tumor necrosis factor-alpha processing activity is tightly controlled by a component that does not affect notch processing. J. Biol. Chem. **273**:24955-24962.

10. **Decoster, E., B. Vanhaesebroeck, P. Vandenabeele, J. Grooten, and W. Fiers**. 1995. Generation and biological characterization of membrane-bound, uncleavable murine tumor necrosis factor. J. Biol. Chem. **270**:18473-18478.

11. 1999. TNF neutralization in MS: results of a randomized, placebo-controlled multicenter study. The Lenercept Multiple Sclerosis Study Group and The University of British Columbia MS/MRI Analysis Group. Neurology **53**:457-465.

12. **Liao, Y. F., B. J. Wang, H. T. Cheng, L. H. Kuo, and M. S. Wolfe**. 2004. Tumor necrosis factor-alpha, interleukin-1beta, and interferon-gamma stimulate gamma-secretase-mediated cleavage of amyloid precursor protein through a JNK-dependent MAPK pathway. J. Biol. Chem. **279**:49523-49532.

13. **Wallach, D., E. E. Varfolomeev, N. L. Malinin, Y. V. Goltsev, A. V. Kovalenko, and M. P. Boldin**. 1999. Tumor necrosis factor receptor and Fas signaling mechanisms. Annu. Rev. Immunol. **17**:331-367.

14. **Mabbott, N. A., G. McGovern, M. Jeffrey, and M. E. Bruce**. 2002. Temporary blockade of the tumor necrosis factor receptor signaling pathway impedes the spread of scrapie to the brain. J. Virol. **76**:5131-5139.

15. **Mabbott, N. A., A. Williams, C. F. Farquhar, M. Pasparakis, G. Kollias, and M. E. Bruce**. 2000. Tumor necrosis factor alpha-deficient, but not interleukin-6-deficient, mice resist peripheral infection with scrapie. J. Virol. **74**:3338-3344.

16. **Rostasy, K., L. Monti, C. Yiannoutsos, J. Wu, J. Bell, J. Hedreen, and B. A. Navia**. 2000. NFkappaB activation, TNF-alpha expression, and apoptosis in the AIDS-Dementia-Complex. J. Neurovirol. **6**:537-543.

17. **Saha, R. N. and K. Pahan**. 2003. Tumor necrosis factor-alpha at the crossroads of neuronal life and death during HIV-associated dementia. J. Neurochem. **86**:1057-1071.

18. **Speth, C., M. P. Dierich, and S. Sopper**. 2005. HIV-infection of the central nervous system: the tightrope walk of innate immunity. Mol. Immunol. **42**:213-228.

19. **Ashkenazi, A.** 2002. Targeting death and decoy receptors of the tumour-necrosis factor superfamily. Nat. Rev. Cancer **2**:420-430.

20. **Shakoor, N., M. Michalska, C. A. Harris, and J. A. Block**. 2002. Drug-induced systemic lupus erythematosus associated with etanercept therapy. Lancet **359**:579-580.

21. **Quasney, M. W., Q. Zhang, S. Sargent, M. Mynatt, J. Glass, and J. McArthur**. 2001. Increased frequency of the tumor necrosis factor-alpha-308 A allele in adults with human immunodeficiency virus dementia. Ann. Neurol. **50**:157-162.

22. **Yeh, M. W., M. Kaul, J. Zheng, H. S. Nottet, M. Thylin, H. E. Gendelman, and S. A. Lipton**. 2000. Cytokine-stimulated, but not HIV-infected, human monocyte-derived macrophages produce neurotoxic levels of l -cysteine. J. Immunol. **164**:4265-4270.

23. **Peschon, J. J., D. S. Torrance, K. L. Stocking, M. B. Glaccum, C. Otten, C. R. Willis, K. Charrier, P. J. Morrissey, C. B. Ware, and K. M. Mohler**. 1998. TNF receptor-deficient mice reveal divergent roles for p55 and p75 in several models of inflammation. J. Immunol. **160**:943-952.

24. **Havenith, C. E., D. Askew, and W. S. Walker**. 1998. Mouse resident microglia: isolation and characterization of immunoregulatory properties with naive CD4+ and CD8+ T-cells. Glia **22**:348-359.

25. **Rothe, M., M. G. Pan, W. J. Henzel, T. M. Ayres, and D. V. Goeddel**. 1995. The TNFR2-TRAF signaling complex contains two novel proteins related to baculoviral inhibitor of apoptosis proteins. Cell **83**:1243-1252.

26. **Choi, C. and E. N. Benveniste**. 2004. Fas ligand/Fas system in the brain: regulator of immune and apoptotic responses. Brain Res. Brain Res. Rev. **44**:65-81.

27. **Choe, W., G. Stoica, W. Lynn, and P. K. Wong**. 1998. Neurodegeneration induced by MoMuLV-ts1 and increased expression of Fas and TNF-alpha in the central nervous system. Brain Res. **779**:1-8.

28. **Elovaara, I., F. Sabri, F. Gray, I. Alafuzoff, and F. Chiodi**. 1999. Upregulated expression of Fas and Fas ligand in brain through the spectrum of HIV-1 infection. Acta Neuropathol. (Berl) **98**:355-362.

29. **Ferrer, I., R. Blanco, B. Cutillas, and S. Ambrosio**. 2000. Fas and Fas-L expression in Huntington's disease and Parkinson's disease. Neuropathol. Appl. Neurobiol. **26**:424-433.

30. **Ferrer, I., B. Puig, J. Krupinsk, M. Carmona, and R. Blanco**. 2001. Fas and Fas ligand expression in Alzheimer's disease. Acta Neuropathol. (Berl) **102**:121-131.

31. **Kuno, R., J. Wang, J. Kawanokuchi, H. Takeuchi, T. Mizuno, and A. Suzumura**. 2005. Autocrine activation of microglia by tumor necrosis factor-alpha. J. Neuroimmunol. **162**:89-96.

32. **Pearse, D. D., F. C. Pereira, A. Stolyarova, D. J. Barakat, and M. B. Bunge**. 2004. Inhibition of tumour necrosis factor-alpha by antisense targeting produces immunophenotypical and morphological changes in injury-activated microglia and macrophages. Eur. J. Neurosci. **20**:3387-3396.

33. **Heise, M. T. and H. W. Virgin**. 1995. The T-cell-independent role of gamma interferon and tumor necrosis factor alpha in macrophage activation during murine cytomegalovirus and herpes simplex virus infections. J. Virol. **69**:904-909.

34. **Vilhardt, F.** 2005. Microglia: phagocyte and glia cell. Int. J. Biochem. Cell Biol. **37**:17-21.

35. **Milner, R. and I. L. Campbell**. 2003. The extracellular matrix and cytokines regulate microglial integrin expression and activation. J. Immunol. **170**:3850-3858.

36. **Albright, A. V. and F. Gonzalez-Scarano**. 2004. Microarray analysis of activated mixed glial (microglia) and monocyte-derived macrophage gene expression. J. Neuroimmunol. **157**:27-38.

37. **Baker, C. A., D. Martin, and L. Manuelidis**. 2002. Microglia from Creutzfeldt-Jakob disease-infected brains are infectious and show specific mRNA activation profiles. J. Virol. **76**:10905-10913.

38. **Baker, C. A. and L. Manuelidis**. 2003. Unique inflammatory RNA profiles of microglia in Creutzfeldt-Jakob disease. Proc. Natl. Acad. Sci. U. S. A **100**:675-679.

39. **Aloisi, F.** 2001. Immune function of microglia. Glia **36**:165-179.

40. **Giese, A., D. R. Brown, M. H. Groschup, C. Feldmann, I. Haist, and H. A. Kretzschmar**. 1998. Role of microglia in neuronal cell death in prion disease. Brain Pathol. **8**:449-457.

41. **Ford, A. L., A. L. Goodsall, W. F. Hickey, and J. D. Sedgwick**. 1995. Normal adult ramified microglia separated from other central nervous system macrophages by flow cytometric sorting. Phenotypic differences defined and direct ex vivo antigen presentation to myelin basic protein-reactive CD4+ T cells compared. J. Immunol. **154**:4309-4321.

42. **Havenith, C. E., D. Askew, and W. S. Walker**. 1998. Mouse resident microglia: isolation and characterization of immunoregulatory properties with naive CD4+ and CD8+ T-cells. Glia **22**:348-359.

43. **Stevens, S. L., J. Bao, J. Hollis, N. S. Lessov, W. M. Clark, and M. P. Stenzel-Poore**. 2002. The use of flow cytometry to evaluate temporal changes in inflammatory cells following focal cerebral ischemia in mice. Brain Res. **932**:110-119.

44. **Williams, A. E., L. J. Lawson, V. H. Perry, and H. Fraser**. 1994. Characterization of the microglial response in murine scrapie. Neuropathol. Appl. Neurobiol. **20**:47-55.

45. **Corbin, M. E., S. Pourciau, T. W. Morgan, M. Boudreaux, and K. E. Peterson**. 2006. Ligand up-regulation does not correlate with a role for CCR1 in pathogenesis in a mouse model of non-lymphocyte-mediated neurological disease. J. Neurovirol. **12**:241-250.

46. **Babcock, A. A., W. A. Kuziel, S. Rivest, and T. Owens**. 2003. Chemokine expression by glial cells directs leukocytes to sites of axonal injury in the CNS. J. Neurosci. **23**:7922-7930.

47. **Havenith, C. E., D. Askew, and W. S. Walker**. 1998. Mouse resident microglia: isolation and characterization of immunoregulatory properties with naive CD4+ and CD8+ T-cells. Glia **22**:348-359.

48. **Cosenza, M. A., M. L. Zhao, Q. Si, and S. C. Lee**. 2002. Human brain parenchymal microglia express CD14 and CD45 and are productively infected by HIV-1 in HIV-1 encephalitis. Brain Pathol. **12**:442-455.

49. **Sanchez-Ramon, S., C. Canto-Nogues, and A. Munoz-Fernandez**. 2002. Reconstructing the course of HIV-1-associated progressive encephalopathy in children. Med. Sci. Monit. **8**:RA249-RA252.

50. **Lipton, S. A. and H. E. Gendelman**. 1995. Seminars in medicine of the Beth Israel Hospital, Boston. Dementia associated with the acquired immunodeficiency syndrome. N. Engl. J. Med. **332**:934-940.

51. **Schwartz, M.** 2003. Macrophages and microglia in central nervous system injury: are they helpful or harmful? J. Cereb. Blood Flow Metab **23**:385-394.

52. **Rogers, J. and L. F. Lue**. 2001. Microglial chemotaxis, activation, and phagocytosis of amyloid beta-peptide as linked phenomena in Alzheimer's disease. Neurochem. Int. **39**:333-340.

53. **Schonrock, L. M., T. Kuhlmann, S. Adler, A. Bitsch, and W. Bruck**. 1998. Identification of glial cell proliferation in early multiple sclerosis lesions. Neuropathol. Appl. Neurobiol. **24**:320-330.

54. **Allen, J. C.** 1976. Minocycline. Ann. Intern. Med. **85**:482-487.

55. **Chopra, I. and M. Roberts**. 2001. Tetracycline antibiotics: mode of action, applications, molecular biology, and epidemiology of bacterial resistance. Microbiol. Mol. Biol. Rev. **65**:232-260.

56. **Teng, Y. D., H. Choi, R. C. Onario, S. Zhu, F. C. Desilets, S. Lan, E. J. Woodard, E. Y. Snyder, M. E. Eichler, and R. M. Friedlander**. 2004. Minocycline inhibits contusion-triggered mitochondrial cytochrome c release and mitigates functional deficits after spinal cord injury. Proc. Natl. Acad. Sci. U. S. A **101**:3071-3076.

57. **Zemke, D. and A. Majid**. 2004. The potential of minocycline for neuroprotection in human neurologic disease. Clin. Neuropharmacol. **27**:293-298.

58. **Ryu, J. K., S. Franciosi, P. Sattayaprasert, S. U. Kim, and J. G. McLarnon**. 2004. Minocycline inhibits neuronal death and glial activation induced by beta-amyloid peptide in rat hippocampus. Glia **48**:85-90.

59. **Yrjanheikki, J., R. Keinanen, M. Pellikka, T. Hokfelt, and J. Koistinaho**. 1998. Tetracyclines inhibit microglial activation and are neuroprotective in global brain ischemia. Proc. Natl. Acad. Sci. U. S. A **95**:15769-15774.

60. **Bantubungi, K., C. Jacquard, A. Greco, A. Pintor, A. Chtarto, K. Tai, M. C. Galas, L. Tenenbaum, N. Deglon, P. Popoli, L. Minghetti, E. Brouillet, J. Brotchi, M. Levivier, S. N. Schiffmann, and D. Blum**. 2005. Minocycline in phenotypic models of Huntington's disease. Neurobiol. Dis. **18**:206-217.

61. **Chen, M., V. O. Ona, M. Li, R. J. Ferrante, K. B. Fink, S. Zhu, J. Bian, L. Guo, L. A. Farrell, S. M. Hersch, W. Hobbs, J. P. Vonsattel, J. H. Cha, and R. M. Friedlander**. 2000. Minocycline inhibits caspase-1 and caspase-3 expression and delays mortality in a transgenic mouse model of Huntington disease. Nat. Med. **6**:797-801.

62. **Wang, X., S. Zhu, M. Drozda, W. Zhang, I. G. Stavrovskaya, E. Cattaneo, R. J. Ferrante, B. S. Kristal, and R. M. Friedlander**. 2003. Minocycline inhibits caspase-independent and -dependent mitochondrial cell death pathways in models of Huntington's disease. Proc. Natl. Acad. Sci. U. S. A **100**:10483-10487.

63. **Zink, M. C., J. Uhrlaub, J. DeWitt, T. Voelker, B. Bullock, J. Mankowski, P. Tarwater, J. Clements, and S. Barber**. 2005. Neuroprotective and anti-human immunodeficiency virus activity of minocycline. JAMA **293**:2003-2011.

64. **Lee, S. M., T. Y. Yune, S. J. Kim, Y. C. Kim, Y. J. Oh, G. J. Markelonis, and T. H. Oh**. 2004. Minocycline inhibits apoptotic cell death via attenuation of TNF-alpha expression following iNOS/NO induction by lipopolysaccharide in neuron/glia co-cultures. J. Neurochem. **91**:568-578.

65. **Tikka, T., B. L. Fiebich, G. Goldsteins, R. Keinanen, and J. Koistinaho**. 2001. Minocycline, a tetracycline derivative, is neuroprotective against excitotoxicity by inhibiting activation and proliferation of microglia. J. Neurosci. **21**:2580-2588.

66. **Tikka, T. M. and J. E. Koistinaho**. 2001. Minocycline provides neuroprotection against N-methyl-D-aspartate neurotoxicity by inhibiting microglia. J. Immunol. **166**:7527-7533.

67. **Peterson, K. E., J. S. Errett, T. Wei, D. E. Dimcheff, R. Ransohoff, W. A. Kuziel, L. Evans, and B. Chesebro**. 2004. MCP-1 and CCR2 contribute to non-lymphocyte-mediated brain disease induced by Fr98 polytropic retrovirus infection in mice: role for astrocytes in retroviral neuropathogenesis. J. Virol. **78**:6449-6458.

68. **Robertson, S. J., K. J. Hasenkrug, B. Chesebro, and J. L. Portis**. 1997. Neurologic disease induced by polytropic murine retroviruses: neurovirulence determined by efficiency of spread to microglial cells. J. Virol. **71**:5287-5294.

69. **Van Hoeven, N. S. and A. D. Miller**. 2005. Use of different but overlapping determinants in a retrovirus receptor accounts for non-reciprocal interference between xenotropic and polytropic murine leukemia viruses. Retrovirology. **2**:76.

70. **Hasenkrug, K. J., S. J. Robertson, J. Porti, F. McAtee, J. Nishio, and B. Chesebro**. 1996. Two separate envelope regions influence induction of brain disease by a polytropic murine retrovirus (FMCF98). J. Virol. **70**:4825-4828.

71. **Portis, J. L., S. Czub, S. Robertson, F. McAtee, and B. Chesebro**. 1995. Characterization of a neurologic disease induced by a polytropic murine retrovirus: evidence for differential targeting of ecotropic and polytropic viruses in the brain. J. Virol. **69**:8070-8075.

72. **Peterson, K. E., S. J. Robertson, J. L. Portis, and B. Chesebro**. 2001. Differences in cytokine and chemokine responses during neurological disease induced by polytropic murine retroviruses Map to separate regions of the viral envelope gene. J. Virol. **75**:2848-2856.

73. **Moore, R. J., D. M. Owens, G. Stamp, C. Arnott, F. Burke, N. East, H. Holdsworth, L. Turner, B. Rollins, M. Pasparakis, G. Kollias, and F. Balkwill**. 1999. Mice deficient in tumor necrosis factor-alpha are resistant to skin carcinogenesis. Nat. Med. **5**:828-831.

74. **Robertson, M. N., M. Miyazawa, S. Mori, B. Caughey, L. H. Evans, S. F. Hayes, and B. Chesebro**. 1991. Production of monoclonal antibodies reactive with a denatured form of the Friend murine leukemia virus gp70 envelope protein: use in a focal infectivity assay, immunohistochemical studies, electron microscopy and western blotting. J. Virol. Methods **34**:255-271.

75. **Havenith, C. E., D. Askew, and W. S. Walker**. 1998. Mouse resident microglia: isolation and characterization of immunoregulatory properties with naive CD4+ and CD8+ T-cells. Glia **22**:348-359.

76. **Walker, W. S., J. Gatewood, E. Olivas, D. Askew, and C. E. Havenith**. 1995. Mouse microglial cell lines differing in constitutive and interferon-gamma-inducible antigen-presenting activities for naive and memory CD4+ and CD8+ T cells. J. Neuroimmunol. **63**:163-174.

77. **Sedgwick, J. D., S. Schwender, H. Imrich, R. Dorries, G. W. Butcher, and M. ter, V**. 1991. Isolation and direct characterization of resident microglial cells from the normal and inflamed central nervous system. Proc. Natl. Acad. Sci. U. S. A **88**:7438-7442.

78. **Stein, V. M., M. Czub, N. Schreiner, P. F. Moore, M. Vandevelde, A. Zurbriggen, and A. Tipold**. 2004. Microglial cell activation in demyelinating canine distemper lesions. J. Neuroimmunol. **153**:122-131.

79. **Williams, K. C. and W. F. Hickey**. 2002. Central nervous system damage, monocytes and macrophages, and neurological disorders in AIDS. Annu. Rev. Neurosci. **25**:537-562.

80. **Matyszak, M. K., S. is-Donini, S. Citterio, R. Longhi, F. Granucci, and P. Ricciardi-Castagnoli**. 1999. Microglia induce myelin basic protein-specific T cell anergy or T cell activation, according to their state of activation. Eur. J. Immunol. **29**:3063-3076.

81. **Richardson-Burns, S. M. and K. L. Tyler**. 2005. Minocycline delays disease onset and mortality in reovirus encephalitis. Exp. Neurol. **192**:331-339.

82. **Pejawar, S. S., G. D. Parks, and M. A. exander-Miller**. 2005. Abortive versus productive viral infection of dendritic cells with a paramyxovirus results in differential upregulation of select costimulatory molecules. J. Virol. **79**:7544-7557.

83. **Zeinstra, E., N. Wilczak, and K. J. De**. 2003. Reactive astrocytes in chronic active lesions of multiple sclerosis express co-stimulatory molecules B7-1 and B7-2. J. Neuroimmunol. **135**:166-171.

84. **Gartner, S.** 2000. HIV infection and dementia. Science **287**:602-604.

85. **Perez, O. D. and G. P. Nolan**. 2001. Resistance is futile: assimilation of cellular machinery by HIV-1. Immunity. **15**:687-690.

86. **Pasparakis, M., L. Alexopoulou, V. Episkopou, and G. Kollias**. 1996. Immune and inflammatory responses in TNF alpha-deficient mice: a critical requirement for TNF alpha in the formation of primary B cell follicles, follicular dendritic cell networks and germinal centers, and in the maturation of the humoral immune response. J. Exp. Med. **184**:1397-1411.

87. **Sriram, K., D. B. Miller, and J. P. O'Callaghan**. 2006. Minocycline attenuates microglial activation but fails to mitigate striatal dopaminergic neurotoxicity: role of tumor necrosis factor-alpha. J. Neurochem. **96**:706-718.

88. **Portis, J. L., S. Czub, C. F. Garon, and F. J. McAtee**. 1990. Neurodegenerative disease induced by the wild mouse ecotropic retrovirus is markedly accelerated by long terminal repeat and gag-pol sequences from nondefective Friend murine leukemia virus. J. Virol. **64**:1648-1656.

89. **Lee, N. K. and S. Y. Lee**. 2002. Modulation of life and death by the tumor necrosis factor receptor-associated factors (TRAFs). J. Biochem. Mol. Biol. **35**:61-66.

90. **Lee, S. Y., A. Reichlin, A. Santana, K. A. Sokol, M. C. Nussenzweig, and Y. Choi**. 1997. TRAF2 is essential for JNK but not NF-kappaB activation and regulates lymphocyte proliferation and survival. Immunity. **7**:703-713.

91. **Tsitsikov, E. N., D. A. Wright, and R. S. Geha**. 1997. CD30 induction of human immunodeficiency virus gene transcription is mediated by TRAF2. Proc. Natl. Acad. Sci. U. S. A **94**:1390-1395.

92. **Landau, A. M., K. C. Luk, M. L. Jones, R. Siegrist-Johnstone, Y. K. Young, E. Kouassi, V. V. Rymar, A. Dagher, A. F. Sadikot, and J. Desbarats**. 2005. Defective Fas expression exacerbates neurotoxicity in a model of Parkinson's disease. J. Exp. Med. **202**:575-581.

93. **Sabelko-Downes, K. A., J. H. Russell, and A. H. Cross**. 1999. Role of Fas--FasL interactions in the pathogenesis and regulation of autoimmune demyelinating disease. J. Neuroimmunol. **100**:42-52.

Vita

Meryll Elizabeth Corbin was born the second of three children to Leslie and Michael Corbin at Melrose-Wakefield Hospital and raised in the quaint town of North Reading, Massachusetts. In high school, she was an avid member of the concert, jazz, marching band and chorus and was president of the North Reading High School Masquer's Club. During the summers she washed dogs at the local groomer where she learned to love all things furry. At the tender age of 17 she went on to study animal science at the University of Massachusetts at Amherst where she graduated *cum laude* in 2004. While at UMass, she became the Area Director for Silver Jewelry at the Student Union Craft Center and was a resident assistant in Orchard Hill for three semesters. After graduation, and not without some trepidation, she made the move to Baton Rouge, Louisiana, where she now resides, to study at the Louisiana State University School of Veterinary Medicine. Although she is unsure of what her next career move will be, she is certain that it will be a rocking good time.